

8 Muon Beamline

8.1 Introduction

The fundamental goal of the Muon Beamline is to deliver a stopped muon rate of approximately a few times 10^{10} per second to the muon stopping target, located in the Detector Solenoid (DS), and to reduce the background in the tracker, calorimeter and cosmic ray veto detectors to a level sufficient to achieve the desired experimental sensitivity (see Chapter 3).

It is important to identify all possible background sources and equip the Muon Beamline vacuum space with elements that can produce a muon beam with the requisite cleanliness while guiding negatively charged muons to the stopping target. The stopping target and the surrounding absorbers must be designed to maximize the capture of muons and transmission of conversion electrons to the detector while minimizing harmful particles that can result in background.

The Muon Beamline is essentially a vacuum space, which serves as a free path for negatively charged muons within the desired momentum range. The muons spiral to the detector area along the streamline of a B-field (created by superconducting solenoid magnets) parallel to the direction of the muons. The S-shaped muon channel is surrounded with coils that form a toroidal B-field in the two curved sections and solenoidal fields in the three straight sections. The upstream toroidal field, with strategically placed collimators, filters the particle flux producing a momentum- and charge-selected muon beam, with good reduction in contamination from positively charged particles: e^\pm , μ^+ , π^\pm , p and neutral particles. A thin Kapton window resides in the central straight section of the Muon Beamline. The window stops antiprotons from reaching the stopping target and creating background. It also serves to separate the upstream and downstream vacuum volumes to prevent radioactive ions or atoms from the production target from contaminating the detector solenoid volume. The muon stopping target consists of thin aluminum discs placed in the detector region of the muon channel in a graded magnetic field. The muons have high efficiency for stopping in the muon stopping target. Muons not stopped in the target mostly bypass the detectors and are transported to the muon beam-stop. Protons and neutrons originating from the muon capture process in the stopping target, final collimator and muon beam stop are attenuated by absorbers to minimize detector background rates.

The Muon Beamline Level 2 system has been divided into 10 Level 3 sub-projects:

- WBS 5.2 Vacuum system
- WBS 5.3 Collimators
- WBS 5.4 Beamline Shielding
- WBS 5.5 Stopping Target
- WBS 5.6 Stopping Target Monitor
- WBS 5.7 Proton Absorber
- WBS 5.8 Muon Beam Stop
- WBS 5.9 Neutron Absorber
- WBS 5.10 Detector Support and Installation
- WBS 5.11 System Integration, Tests and Analysis

In Section 8.2 the requirements for the Muon Beamline are presented. In Section 8.3 the proposed design and the alternatives to the proposed design are discussed. In Section 8.4 Risk Management for the Muon Beamline is described. Section 8.5 discusses Quality Assurance, Value Management is described in Section 8.6, ES&H is discussed in Section 8.7 and the Muon Beamline R&D plan is described in Section 8.8.

8.2 Requirements

In this section the overall requirements for the Muon Beamline are described. A detailed description of the requirements for each Level 3 deliverable can be found in the various Requirements & Specifications documents [1] - [10].

8.2.1 Vacuum System

A detailed description of the requirements and specifications for the Mu2e vacuum system can be found in [1].

The Muon Beamline must be under vacuum. There are a number of factors, listed below, that must be considered to determine the requirement on vacuum system pressure.

- The muon beam must be efficiently transported from the production area to the stopping target with minimum loss of the muons in the momentum range below 50 MeV/c.
- The background rate from beam particles scattering off residual gas molecules shall be less than the background generated by electrons from muon decays in orbit.
- The vacuum level must be below the Townsend limit to prevent electrical discharge from detector high voltage.

- Multiple scattering and energy loss must be minimized for conversion electrons to limit the overall contribution to the energy resolution of the Tracker to less than 10 keV, which is negligible compared to the required Tracker resolution.

It has been shown that by keeping the vacuum $\leq 10^{-4}$ Torr for the downstream vacuum volume the physics requirements can be met [1]. Consequently we require 10^{-4} Torr or lower pressure at the downstream part of the vacuum volume for the Muon Beamline. For the upstream part of the vacuum volume $\leq 10^{-1}$ Torr pressure is sufficient.

The detector vacuum volume must be isolated from the upstream part of the beamline to prevent migration of radioactive molecules generated at the production target area to the detector area.

The vacuum system includes a closure at the upstream end of the Production Solenoid. The closure shall contain a vacuum window to allow beam protons that are not absorbed by the production target to exit the PS. The Proton Beam Exit window will also serve as the Extinction Monitor window. Another vacuum window will be incorporated into Production Target Extraction port, centered on the solenoid axis, for target insertion/removal via remote handling. An additional port for a radiation-hard camera will allow safe visual monitoring of the production target. The vacuum closure must also provide a vacuum pump duct. The duct must have a conductance that is suitable to provide the required evacuation when the vacuum pumps are located some distance away in regions that allows adequate shielding from radiation and magnetic fields.

The Detector Solenoid vacuum enclosure must support all signal, power, high-voltage, detector gas and cooling lines from the interior of the DS to the outside. Furthermore, the enclosure must accommodate the muon beam stop so that it may lie in the region where the magnetic field falls to zero; this prevents many charged particles from returning upstream towards the detectors. The DS vacuum enclosure requires a thin window at its center for the muon stopping target monitor system.

The vacuum system must work in concert with the detector high voltage (HV) distribution systems to either isolate the HV from the vacuum or ensure that the HV is turned off before sparks occur in the event of a sudden vacuum loss.

The pump down time is to be of order several hours so as not to significantly impact experimental operations.

8.2.2 Collimators

The Muon Beamline must be equipped with collimators to define the muon beam and a thin window to absorb antiprotons. The collimators are required to perform a number of functions.

- Select the charge and momentum range of particles. The muon beam line suppression of electrons (the ratio of electrons that enter to the TS to the number that traverse the muon beam line and enter to the DS) with energies above 100 MeV needs to be a factor of 1×10^6 or better. The probability for particles with the wrong charge to pass through the central collimator (COL3) must be less than 2% for every proton that hits the production target.
- Antiprotons must be absorbed in a thin window located between TSu and TSd. The annihilation products must be absorbed in the collimation system before reaching the Detector Solenoid. The antiproton window must also prevent radioactive molecules from migrating from the production target region to the Detector Solenoid. The window must be thick enough to prevent antiproton transmission and molecules migrating through the window. On the other hand, the window needs to be thin enough to attenuate the muon yield by no more than 15%.
- The detectors should be shielded from neutrons and low momentum muons that do not hit the stopping target.
- The heat load in the Transport Solenoid coils from particle debris originating from the production target must be minimized. The peak power density deposited into the TS coils must be less than $5 \mu\text{W/g}$ at the highest proton beam intensity.

A detailed description of the requirements and specifications for the Collimators can be found in [2].

8.2.3 Muon Beamline Shielding

The S-shaped Transport Solenoid filters unwanted charged and neutral particles from the beam. Shielding might be required both inside and outside the Transport Solenoid to further reduce the yield of neutral particles wandering downstream (like thermal neutrons) and to shield the superconducting coils. An intense neutral particle beam hits the first curved section of the Transport Solenoid. It is necessary to reduce the thermal load in the superconducting coils to less than $5 \mu\text{W/g}$ at any point within the coil volume. A detailed description of the requirements and specifications for the Muon Beamline Shielding can be found in [3].

8.2.4 Muon Stopping Target

The stopping target material, shape and location must be chosen to stop as many muons as needed ($\sim 10^{18}$) while minimizing the energy loss and maximizing the acceptance for conversion electrons. The stopping target requirements are strongly coupled to the choice of the experimental layout (B-field requirements, Tracker and Calorimeter design and placement, neutron and proton absorbers design and placement etc.). The detailed description of the requirements and specification that takes into account the current Mu2e design is described in [4].

8.2.5 Muon Stopping Target Monitor

A Muon Stopping Target Monitor is required to measure the muon stopping rate during the live time of the experiment by measuring the characteristic X-ray spectrum from the muon atomic cascade process. The capture rate is derived from the stopping rate. The requirement is to achieve a measurement accuracy of 10%. The actual choice of the measurement technique strongly depends on the experimental layout (target material choice, dimension and location, possible locations for the monitor etc.). The detailed description of the requirements and specifications that takes into account the current Mu2e design is described in [5].

8.2.6 Proton Absorber

Protons that result from muon captures on target nuclei in the muon stopping target can negatively impact the performance of the tracker and the calorimeter and possibly lead to backgrounds. The proton absorber must meet the following three requirements:

- Reduce the rate of stopping target protons that reach the tracker to a level where reconstruction of electron tracks is reliable and robust. For the current tracker design this rate is 60 kHz.
- Minimize the energy loss and multiple scattering of conversion electron candidates at 105 MeV that pass through the proton absorber below 300 keV.
- Ensure by the shape and location of the proton absorber that muons do not stop on the proton absorber.

The first two requirements end to work contrary to one another. A thicker absorber will stop more protons but will further degrade the momentum resolution. A detailed optimization of the stopping target, absorbers and tracker is required to finalize the proton absorber design. Further detailed requirements and specifications for the Proton Absorber can be found in [6].

8.2.7 Muon Beam Stop

The Muon Beamline must be equipped with a Muon Beam Stop to absorb the energy of secondary beam particles (primarily muons and electrons) that reach the end of the Detector Solenoid to reduce the background to the detectors from the muon decays and captures in the beam stop. This is especially important during the detector live-time, which begins about 700 ns after the proton micro bunch hits the target. Near the downstream end of the Detector Solenoid the uniform field transitions to a graded field that drops off along the beam direction; this is a critical feature of the muon beam stop. The field gradient reflects most low energy charged particles produced in the beam stop away from the detectors. A detailed description of the requirements and specifications for the Muon Beam Stop can be found in [7].

8.2.8 Neutron Absorbers

Cosmic rays can cause backgrounds and must be vetoed (Section 3.5.9). A Cosmic Ray Veto (CRV) has been designed for Mu2e that surrounds the Detector Solenoid. The CRV must operate in an environment rich with neutrons from the production target, the final collimator in the Transport Solenoid, the muon stopping target and the muon beam stop. About 1.2 neutrons are produced for each muon that undergoes nuclear capture in the muon stopping target. The neutrons range from thermal to a few tens of MeV. Neutrons from the production target and muon beam transport must be shielded to below the rate of neutrons from muon capture in the stopping target. The preferred alternative design for the CRV is a detector sensitive to these neutrons (scintillator), though the pattern of energy deposition in the multiple layers of active detector will be distinct from cosmic ray muons in most cases. Sufficient absorbing material must be introduced to reduce the overall rate in the CRV and to limit the number of neutrons mistaken for muons.

Neutrons that result from muon captures on target nuclei in the muon stopping target can negatively impact the performance of the tracker and the calorimeter and possibly lead to backgrounds. Further simulations are needed to show whether it is required to place Neutron absorbers in the Detector Solenoid bore together with the muon beam stop to reduce the accidental hits to 6×10^6 hits/sec/m² in the tracker.

The Stopping Target Monitor is sensitive to radiation damage caused by neutrons emerging from the muon stopping target, the production target and the beam stop. It is important to reduce this neutron rate to be able to operate the detector for at least a month continuously without annealing the detector crystals. We anticipate having two detectors so that one is in operation when the other is being annealed.

A detailed description of the requirements and specifications for the Neutron absorbers can be found in [8].

8.2.9 Detector Support and Installation System

The Detector Support Structure is required to transport and align components within the Detector Solenoid warm bore. The muon stopping target, proton absorber, tracker, calorimeter, and muon beam stop must all be moved into position and aligned to the standard Mu2e coordinate system. The components vary significantly in mass (from less than 160 g to over 4000 kg) as well as required alignment accuracy. These components must be supported by the inside wall of the Detector Solenoid cryostat and be moved accurately and safely inside the bore. Physics requirements dictate the overall size, location and placement accuracy of the individual components within the DS bore. In addition, the support structure must not impede particle trajectories or lead to an enhancement of detector rates or physics background as a result of interacting particles. A detailed description of the requirements and specifications for the Detector Support Structure can be found in [9].

8.3 Proposed Design

8.3.1 Vacuum System

The Beamline Vacuum system consists of two distinct vacuum volumes, an upstream volume labeled PS + TSu and a downstream volume labeled TSd + DS. A sealed vacuum window located between Transport Solenoid sections physically separates the two volumes. The vacuum window also serves to stop antiprotons that can lead to a dangerous physics background. The vacuum volume is defined by the inner cryostat walls of the various solenoids, the Production Solenoid enclosure on the upstream end, and the Detector Solenoid enclosure on the downstream end. Connections between solenoids are made with flexible bellows.

The two vacuum volumes are connected by a bypass valve that only opens during pump down or vacuum loss to minimize the pressure differential across the vacuum window.

Not all components of the vacuum system will be ASME code stamped, but they will be designed and manufactured according to the 2010 ASME Boiler and Pressure Vessel Code Section VIII. All components will also be designed according to the standards of the Fermilab Engineering and ES&H Manuals, particularly Vacuum Vessel Safety chapter 5033.

The Production Solenoid Vacuum Enclosure, shown in Figure 8.1, is a 316L stainless steel weldment bolted directly to the upstream end of the PS cryostat. It closes the PS + TSu vacuum volume, provides a place to connect vacuum pumps and provides openings and mounting locations for several PS vacuum windows and feed-throughs.

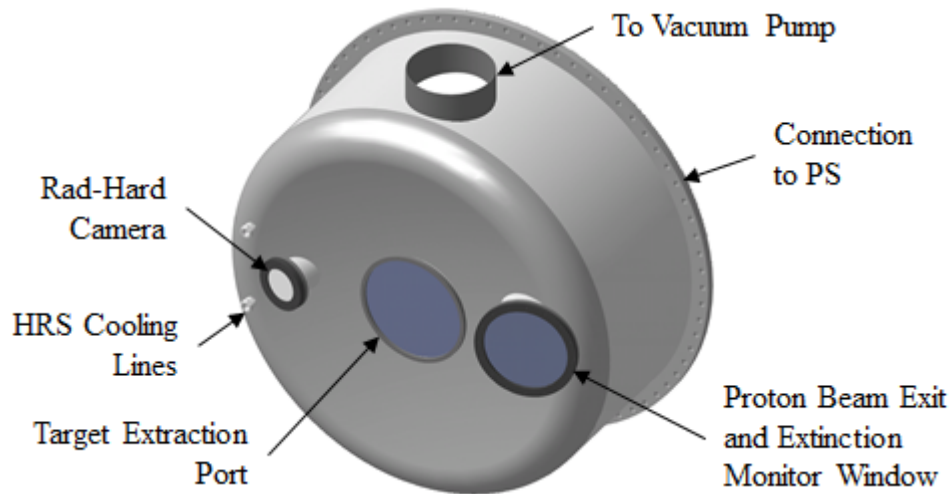


Figure 8.1. Model of the vacuum enclosure on the upstream end of the Production Solenoid (PS) showing the vacuum pump piping, windows, and feedthroughs.

Radiation levels in the Production Solenoid are expected to be high enough to require metal vacuum seals at all locations. One 406.4 mm port with circular cross-section is provided to connect to vacuum and roughing pumps located some distance away. Two 34.93 mm diameter feed-throughs are provided for water cooling lines for the Production Solenoid Heat and Radiation Shield (HRS).

The proton beam exit and extinction monitor window is 400 mm diameter \times 2.84 mm thick Grade 5 titanium. The window for a radiation hard camera is 200 mm diameter \times 25.4 mm thick fused quartz. The target extraction window is 500 mm diameter \times 3.58 mm thick Grade 5 titanium incorporated into the design of the Production Target extraction port. After activation, remote handling equipment will access the production target through this port, should a replacement be required.

The Detector Solenoid Vacuum Enclosure, shown in Figure 8.2, is a two-piece 316L stainless steel weldment bolted directly to the downstream end of the DS cryostat to close the TSd + DS vacuum volume. The Vacuum Pump Spool Piece (VPSP) bolts directly to the downstream end of the DS cryostat and remains fixed, becoming an extension of the cryostat and the internal rail system. Four 406.4 mm diameter flanged ports are provided for direct connection of vacuum pumps and four

304.8 mm diameter ports are available to connect to roughing pumps located some distance away.

The removable Instrumentation Feed-Through Bulkhead (IFB) provides an opening and mounting location for a Stopping Target Monitor (STM) vacuum window. The STM window is 100 mm diameter \times 1.09 mm thick 316L stainless steel. The IFB also provides an axial connection for the Muon Beam Stop (MBS) and a feed-through area for the many cables, gas lines, and cooling lines for the detectors mounted inside the Detector Solenoid. Metal seals will be used for the large diameter connections, but radiation levels in this region are expected to be low enough to allow O-ring seals on feed-throughs.

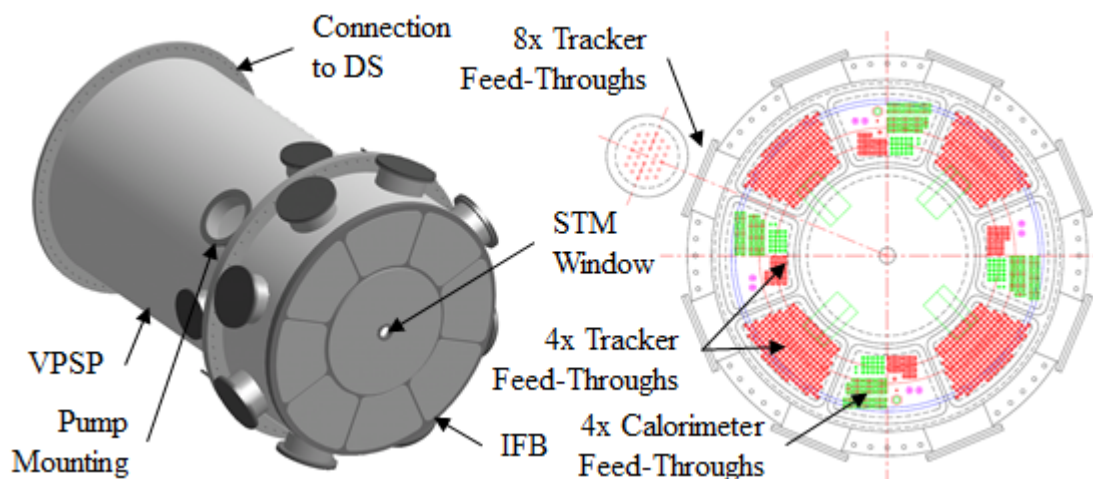


Figure 8.2. Model of the vacuum enclosure on the downstream end of the Detector Solenoid (DS) showing the vacuum pump mounting ports and window. Layout of the downstream end of the Instrumentation Feed-Through Bulkhead showing all Tracker, Calorimeter, and Solenoid feed-throughs.

The Transport Solenoid interconnects, to the Production Solenoid at one end and the Detector Solenoid at the other end, are accomplished by flanged, bolted connections as shown in Figure 8.3. Bellows are built into these connections to allow movement of the TS relative to the PS and DS. Metal seals will be used in these large diameter connections.

The interconnects between the Transport Solenoid sections and the antiproton stopping window module are accomplished by flanged, bolted connections as shown in Figure 8.4. Metal seals will be used in these large diameter connections.

The antiproton stopping window module is designed to be removable for service or replacement, and a bellows is built into this connection design to facilitate this.

Because the space between TSu and TSd is limited, appropriate fixturing and handling equipment will be provided to protect the window, seals, and sealing surfaces during this process.

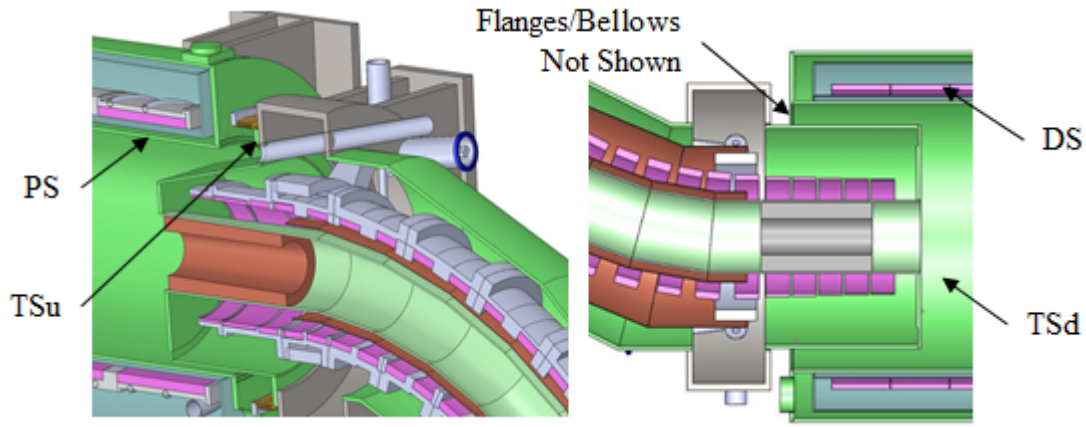


Figure 8.3. Models of the connection of the first Transport Solenoid section (TSu) to the Production Solenoid (PS), and the connection of the last Transport Solenoid section (TSd) to the Detector Solenoid (DS).

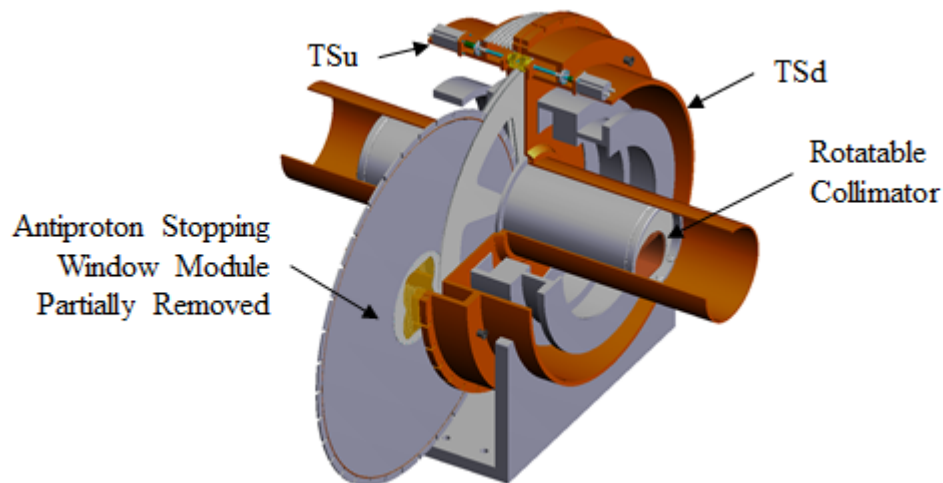


Figure 8.4. Models of the connection of the Transport Solenoid sections (TSu and TSd) to the Antiproton Stopping Window Module.

The flanges welded onto TSu and TSd must accommodate the collimator rotating mechanism, as well as the bypass piping necessary to maintain the 1 torr or less pressure differential across the antiproton stopping window. A design concept for the bypass piping is shown in Figure 8.5. A control system will be required to safely

operate the bypass system and protect the antiproton stopping window from pressure damage.

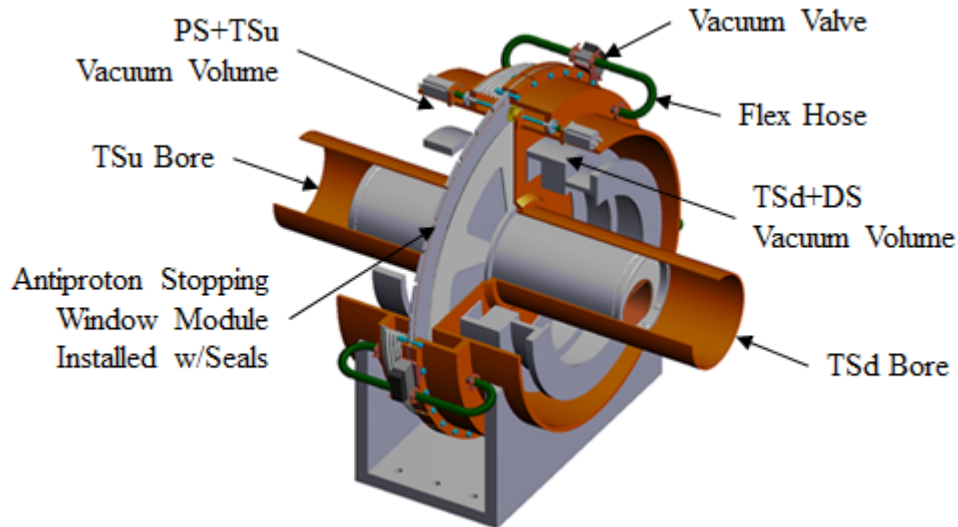


Figure 8.5. Model showing the proposed method of protecting the Antiproton Stopping Window from pressure differential using a system of bypass pipes and control valves.

Identification of the appropriate gas loads, establishment of the specific vacuum equipment, specification of appropriate materials, and definition of interfaces are all factors in selecting the external vacuum system components. To satisfy the requirements the nominal pressure in the detector solenoid must be adjustable from 10^{-4} to $\sim 10^{-5}$ Torr. Gas loads are the most difficult factor to predict in a system like the Mu2e Beamline. Therefore, the design allows for a flexible pumping capacity, incorporating appropriate sensors, pumps, ducts, valves and gas abatement with function, assembly, installation, decommissioning, and ES&H requirements in mind.

The two vacuum volumes share the same dry screw roughing pump. Each vacuum volume has a magnetic levitated hybrid viscous drag-turbo molecular pump to speed the transition to base pressure. Gate valves are located across the intake and exhaust of each high vacuum pump. Pressure sensors are mounted between the gate valves and pumps, near each pump intake.

Materials under vacuum in the PS + TSu volume include copper, brass, tungsten, and stainless steel and the TSd + DS volume contains Kapton, stainless steel, copper, lead, aluminium, lead tungstate crystal, and polyethylene. Nearly every surface of the PS + TSu volume is metal; however, the heat and radiation shield has some obscured surfaces and may turn out to be a minor source of virtual leaks. The challenge to pumping down the PS + TSu volume will simply be the pump-volume distance. Vacuum equipment for the PS + TSu volume must be located far from the intense

radiation and strong magnetic field near the Production Solenoid leading to longer ducts and reduced effective pumping speed. In the TSd + DS volume, material outgassing will present a significant load for the first ten hours at base pressure, then the dominant load will be steady-state leaks from the tracker.

A partial description of the gas loads in the TSd + DS volume has been compiled. The pump-vacuum vessel distance for PS + TSu is driven by the need to protect the equipment from the radiation and magnetic fields present. The DS vacuum volume has two cryo pumps: one for normal operation and one spare that also operates as a backup pump during regeneration. While gas loads in the PS + TSu volume are dominated by transient outgassing from all metal surfaces, the TSd + DS volume is filled with materials that will outgas significantly. The gas loads in the TSd + DS volume will also include leaks from the large number of feed-throughs required in the DS Vacuum Enclosure as well as the tracker gas distribution system and straw end fittings. If the rates in the detectors from scattering on gas atoms require adjustment (e.g., reducing the vacuum level below 10^{-4} Torr), then another pump may be necessary. This risk is mitigated by the inclusion of a third high vacuum pump for the DS.

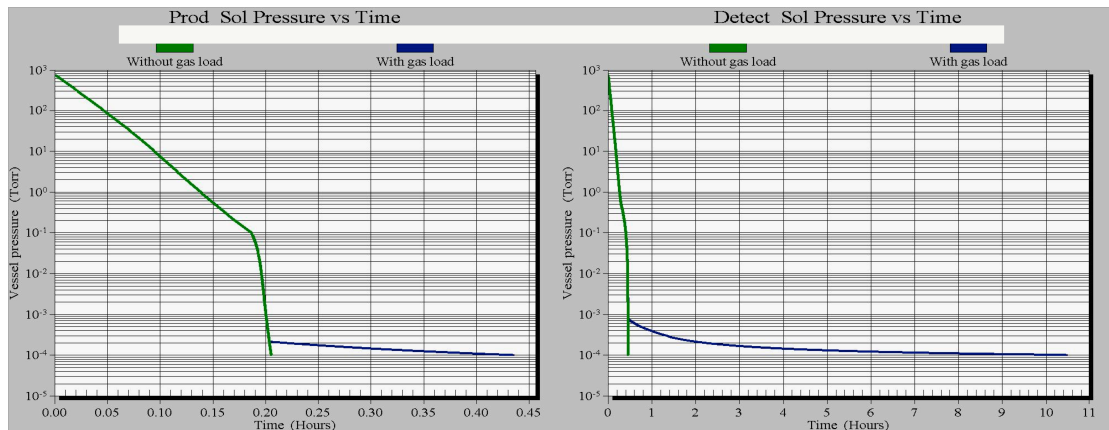


Figure 8.6. Pump down for Mu2e. The current calculated outgas rate only includes all surfaces are assumed prepared to minimize outgassing and considered un-obscured, the maximum tracker leak rate, and displacement volumes we have already designed for Mu2e.

The pump down performance is shown in Figure 8.6. A Kinney SDV 800 roughing pump services both volumes. Each volume has its own Shimadzu Magnetically Levitated Hybrid Molecular Drag/Turbo-Molecular pump model TMP-1003LM and three CTI – Cryogenics (Helix Technologies) model 400 high vacuum cryo pumps. The effective pumping speed of a single cryo-pump attached to the TSd + DS volume is determined from the conductance of the ports attached to the vacuum spool piece.

- Cryo-Torr CTI-400, 6000 l/s
- Orifice, 14,144 l/s
- VAT 16" pneumatic gate valve, 47,638 l/s
- 16" circular duct, 37,803 l/s.

Combining the above information results in a required effective pumping speed of 3509 l/s. At the DS base pressure, the selected cryo pump model can move 0.35 Torr l/s of air [14]. The current estimate of gas loads for this volume is 0.12 Torr litre/sec, so as the gas load estimate becomes more refined it may be possible to eliminate at least one cryo pump or substitute smaller capacity, less expensive pumps.

The effective pumping speed of a single turbo pump servicing the PS + TSu volume is determined as above. Although the PS+TSu vacuum only requires a modest pressure, 0.1 Torr, the turbo-molecular drag hybrid selected can attain pressures just above 10^{-4} Torr quickly. Hence, the estimates for the PS vacuum performance uses this as the upstream base pressure. We make the conservative estimate that the PS + TSu pump will be approximately 6 m away from the PS vacuum ports, behind shielding. The estimated distance has at least a 50% uncertainty. The conductance is estimated using the following input:

- TMP1003LM, 1100 l/s
- Orifice, 14,144 l/s
- VAT 16" pneumatic gate valve, 47,638 l/s
- 16" circular duct, 1453 l/s.

Combining this information gives an effective pumping speed of 592 l/s for a single turbo-pump. At base pressure, the pump moves 0.06 Torr litres/sec in the PS + TSu volume. The gas loads for this volume are estimated to be less than 0.08 Torr l/s [14]. The gas load and pumping rate are comparable in size; as we shall see in Figure 8.6, this poses no challenge to turbo pump operation. However, the required duct length could be much longer and the conductance correspondingly lower. Hence, the PS vacuum closure can accommodate addition pumps and ducts if necessary.

The pump down performance for both vacuum volumes was calculated using VacTran, a commercial vacuum simulation program. Figure 8.6 shows the pump down performance of each volume with a Kinney SDV 800 pump. PS + TSu required 5.5 minutes to reach approximately 10 Torr and TSd + DS required about 10 minutes to reach the same pressure. At 10 Torr the TMP1003 turbo pump is turned on and the SDV 800 is switched off. In the DS vacuum system, the TMP1003 runs for

approximately 20-30 minutes, as seen in Figure 8.6, to reach the crossover region for the cryo pumps. Once the cryo pumps are switched on, the turbo pump is deactivated. At that point, the PS + TSu volume reaches the desired 10^{-4} Torr level in about 12 minutes while the TSd + DS volume requires about 10.5 hours.

During all phases of the pump down (as well as the process of coming up to atmospheric pressure), it is critical that the pressure differential across the antiproton Stopping/Vacuum Window located between TSu and TSd never rise to a value greater than 50 Torr. The window is at significant risk if a leak develops that causes a huge pressure rise and large pressure differences across the window over a short time period. Another significant risk is present during the time of initial pump down. Uncontrolled pump-down speed could exert viscous drag forces on fragile components in the vacuum volumes, particularly in the Detector Solenoid.

The strategy during initial pump down calls for two pressure control valves that are actuated by a control algorithm residing in a Programmable Logic Controller (PLC) used to control and monitor all of the Beamline Vacuum System instrumentation. The algorithm will monitor the measured vacuum pressure in the Production and Detector Solenoids. Since the conductance paths to the two areas are not identical, it is critical that the pressure control valves be stepped from closed to open in a manner that allows for pump down of the entire mass to be as uniform as feasible. The algorithm will adjust each pressure control valve to maintain a constant profile. During the initial pump down stage, valves bypassing the antiproton/vacuum window volume will be open to reduce the risk of a large differential pressure.

The differential pressure (dP) across the antiproton/vacuum window must be maintained below approximately 50 Torr. This dP is approximately 12.5% of the yield point of the window. When the pressure differential across the window is less than 1 Torr, as measured by pressure transducers in the Production and Detector Solenoids, the pressure control valves can be fully opened and the bypass valves across the window may be closed.

Considered Alternatives to the Proposed Design of the Vacuum System

The PS Enclosure may be designed using a thick flat plate instead of an elliptical reverse-domed head. The flat plate design would simplify the vacuum window design and mounting scheme, but would retain higher activation levels from the proton beam.

If verified by gas load studies, the Vacuum Pump Spool Piece may be rotated 45° to allow mounting four 304.8 mm diameter vacuum pumps and gate valves instead of

406.4 mm diameter pumps and valves, resulting in a significant cost savings. At the present time, calculations show that 406.4 mm diameter equipment is required to handle the large amount of material outgassing within the Detector Solenoid.

A faceted Instrumentation Feed-Through Bulkhead (IFB) design made from aluminum plate may be considered. This design would save considerable weight and may minimize the support structure necessary to hold up the Detector Solenoid Vacuum Enclosure to avoid stressing the DS cryostat inner shell. The disadvantage of this faceted IFB is its manufacturability, requiring 100 mm thick aluminum plate to be mitered and welded while maintaining vacuum integrity and ASME code compliance.

8.3.2 Collimators

There are two types of collimator assembly configurations. The first type is a relatively simple collimator (Figure 8.7) that will be used for COL1 and COL5, the collimators in the first and last straight sections of the upstream (TSu) and downstream (TSd) Transport Solenoid. COL1 and COL5 are essentially copper (COL1 has an additional 10 mm graphite liner – inner tube) tubes with a flange and insertion rollers. They are about one meter long with a 0.48 m outer diameter. COL1 bore has 0.3 m and the COL 5 bore has a 0.256 m inner diameter. COL1 may require active cooling and monitoring to control heating that results from the radiation load due to its proximity to the production target. A radial gap of 1-2 mm will be provided between the ID of the cryostat bore and the OD of the collimators to allow for insertion during assembly. COL1 and COL5 (Figure 8.7) are permanently installed. These collimators are not required to be accessible or repairable during the lifetime of the experiment. The flanges will be bolted to the cryostat to prevent axial motion, particularly during a quench when eddy currents may be induced in the collimators that lead to axial forces. The location of the various collimators is shown in Figure 8.8.

The detector area is required to be shielded from neutrons. In addition to its role in collimating the muon beam, the neutron rate is an important consideration in the design of COL5. COL5 could be made from polyethylene or a combination of polyethylene and a high Z material for better neutron absorption. The high Z material will also help to reduce background from beam electrons.

The central straight sections of TSu and TSd contain two collimators, COL3u and COL3d, which rotate (see Figure 8.9 and Figure 8.10). The antiproton stopping window module is located in between TSu and TSd cryostats and must have collimators on both sides, necessitating two rotating collimators rather than just one.

The collimator downstream of the antiproton window is necessary to absorb annihilation products from the interaction of antiprotons in the window. The upstream collimator absorbs higher momentum antiprotons that might otherwise penetrate the window and make their way to the Detector Solenoid.

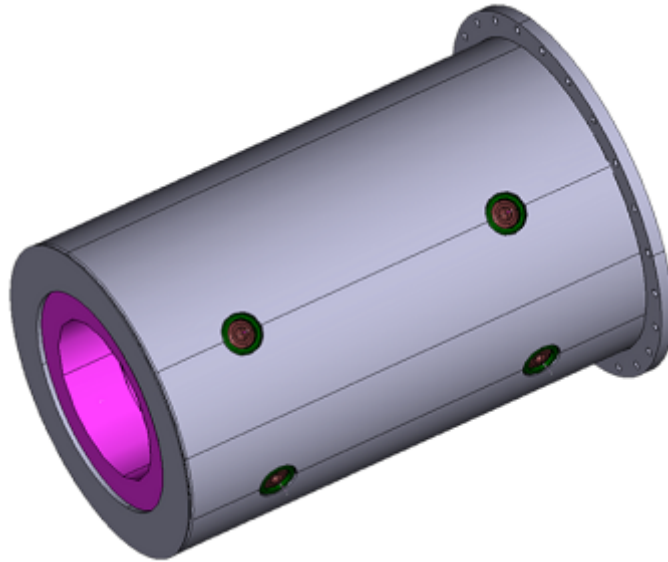


Figure 8.7. 3-D model view of the collimator (COL1 & COL5).

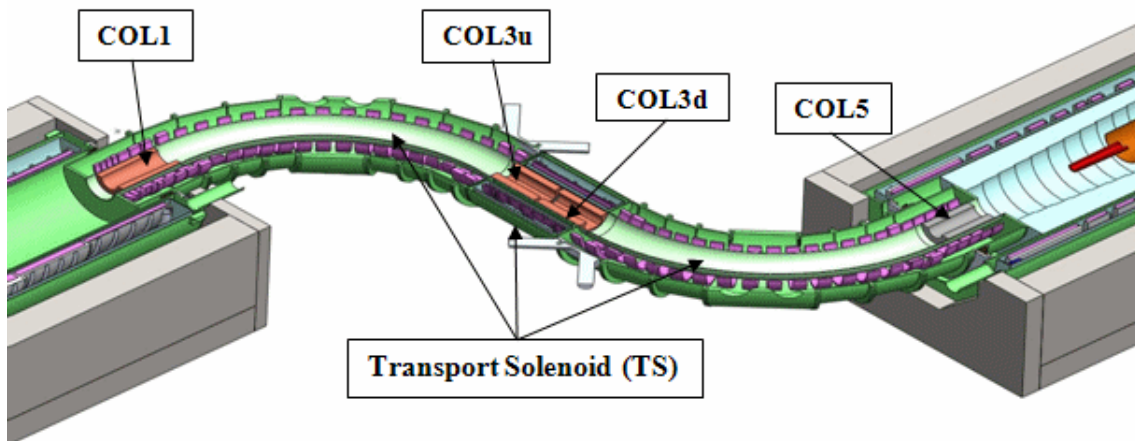


Figure 8.8. Overview of the collimators positioned within the warm bore of the Mu2e Transport Solenoid.

COL3u and COL3d each consist of two major components:

- A stainless steel container with a flange for the connection with the TSu or TSd cryostat flanges. This container will have axial insertion rollers similar to COL1 and COL5 for insertion in the cryostat.

- A copper collimator body with an asymmetric clear bore shown in Figure 8.9. This asymmetric bore provides charge and momentum selection. The collimator will allow passage of low momentum negative particles (or positive particles if the collimators are rotated 180 degrees) while strongly suppressing positives (or negatives). The collimator bodies have bearings to allow 180-degree rotation inside the stainless steel container for detector calibration using μ^+ decays (reference). The rotation mechanism consists of a large gear that is attached to the collimator body (shown in figure 8.9).

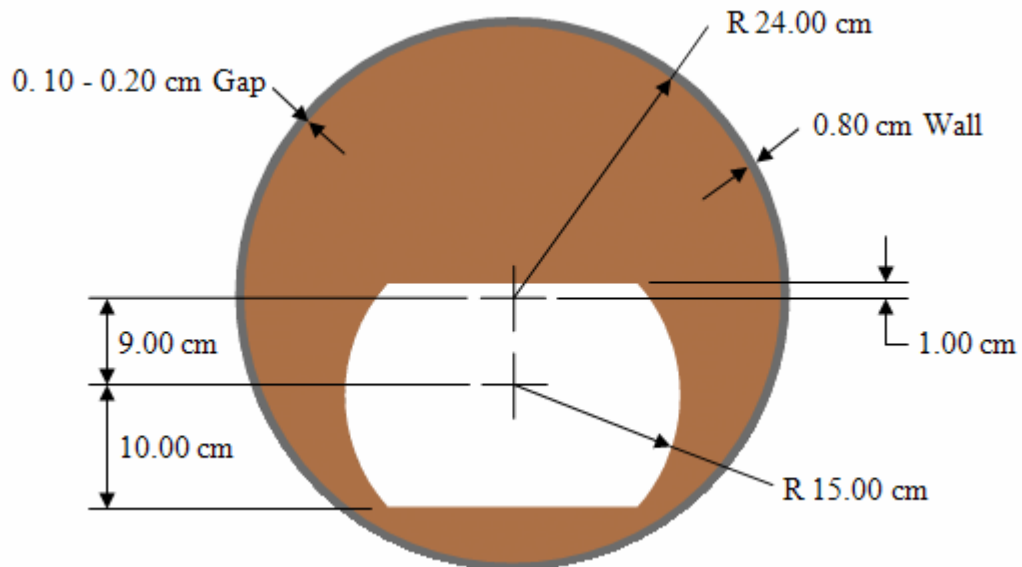


Figure 8.9. Cross-sectional view of the central collimators COL3u and COL3d.

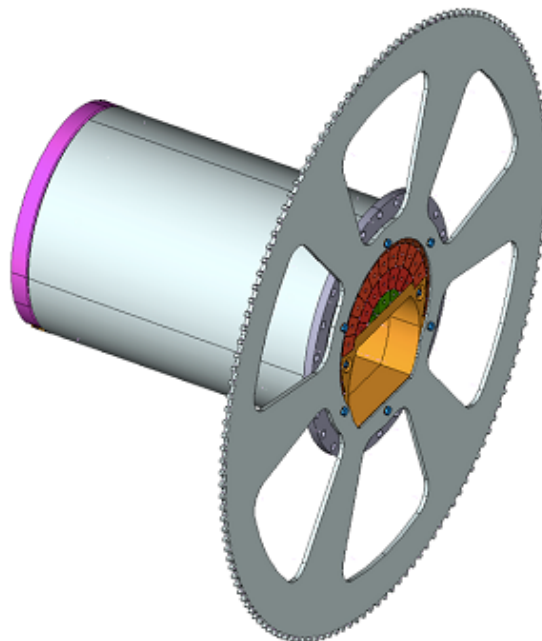


Figure 8.10. Schematic view of the COL3u collimator.

A section view through the TSu and TSd straight sections, including the rotatable collimators, is shown in Figure 8.11. The collimators (COL3u and COL3d) will be supported by the inner tube of the TSu and TSd cryostats and installed during TS assembly. The insertion clearance between the OD of each collimator and the inner TS cryostat wall is 1-2 mm radially. Tolerances for collimator positioning are ± 1 mm inside the cryostat bore. Two rows of bearings will be used to support the collimator body inside the container and provide easy azimuthal rotation inside the container tube. Rotation will be provided by an electrical motor, that will electronically control the orientation of the collimators. There is a 50 mm gap between TSu and TSd cryostats. This gap will provide sufficient room for the two large gears and for the thin antiproton stopping window module that is located in the center of the gap. There will be two drive shafts. Each drive shaft will be rotated by a servomotor. The other end of the drive shaft has a smaller gear that is in connection with the larger gear. Each collimator can be rotated separately.

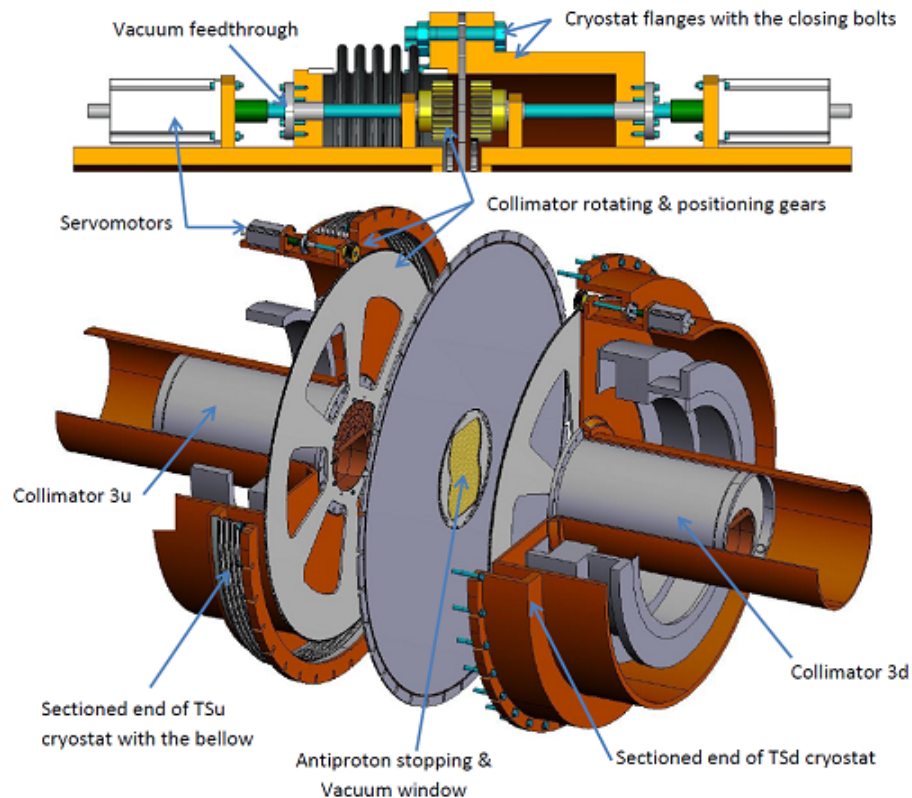


Figure 8.11. Conceptual section view through the TSu and TSd straight sections, antiproton stopping window module, and rotatable collimators.

The antiproton stopping window module will be located in the center of the TS solenoid bore (see Figure 8.11). The window support structure must provide adequate vacuum seals to isolate the upstream and downstream vacuum volumes and also

isolates the vacuum volumes from atmospheric pressure. This will be accomplished by large diameter seals between the window plate and the cryostat flanges. To be able to install/remove the antiproton stopping window module requires breaking the vacuum seal and creating a ~ 5 mm gap. This can be achieved by installing a bellows on one side of the joint. The antiproton stopping window must be made from low-Z material (for example, from Kapton) with a thickness of about 0.67 mm.

The effectiveness of the collimators to select muons of the appropriate charge sign and reduce wrong sign muons is shown in Figure 8.12 and Figure 8.13. In Figure 8.12 the upper curve is the spectrum of negatively charged muons as they exit the Production Solenoid and are incident on the collimation system. The lower curve is the spectrum of negatively charged muons that emerge from the collimation system and enter the Detector Solenoid. Low energy muons with a high probability to stop in the muon stopping target are preferentially selected. In Figure 8.13 the same plot appears for positively charged muons, whose rate is significantly attenuated by the time they reach the Detector Solenoid.

Considered Alternatives to the Proposed Design

Alternatives exist for the composition of COL5, which could be made from polyethylene or a mixture of copper and polyethylene. Additional simulations, optimization of the muon beam, and further studies of backgrounds are required before these alternatives can be fully evaluated.

An alternative design for COL3 has been considered which incorporates a movable central block as shown in Figure 8.14. This design allows fine-tuning of the collimator aperture and might be an advantage during the experiment run time.

Both collimator alternatives described above are mechanically and technologically feasible. More information can be found in the Requirements and Specifications document for the collimators [2].

8.3.3 Muon Beamline Shielding

The heating of the Transport Solenoid coils and other structures is due to primary radiation from the production target and secondary production on the collimators. The Internal Muon Beamline Shield shall limit the instantaneous local heating (as described in [3]) in the Transport Solenoid coils. Simulation shows that the heating is sufficiently low that no internal shielding will be required.

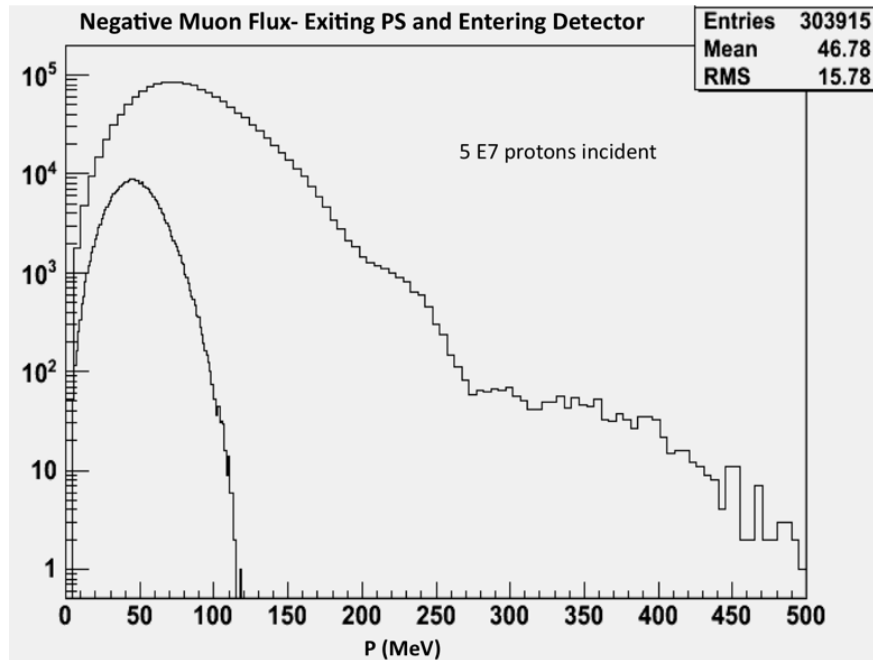


Figure 8.12. The momentum spectrum of negative muons exiting the Production Solenoid and incident on the collimation system (upper curve) and the momentum spectrum of the negatively charged muons that emerge from the collimation system and enter the Detector Solenoid (lower curve).

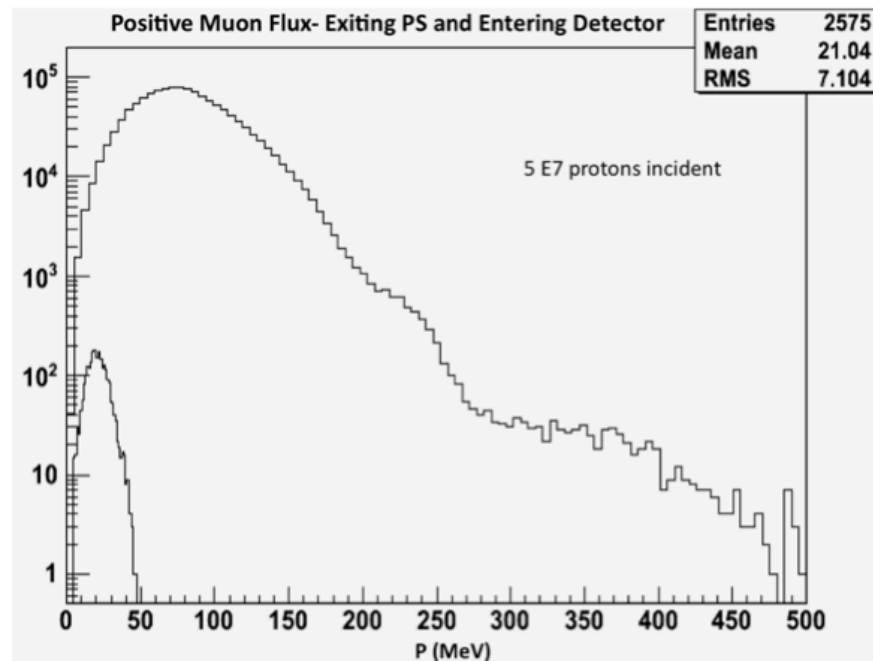


Figure 8.13. The momentum spectrum of positive muons exiting the Production Solenoid and incident on the collimation system (upper curve) and the momentum spectrum of the positively charged muons that emerge from the collimation system and enter the Detector Solenoid (lower curve).

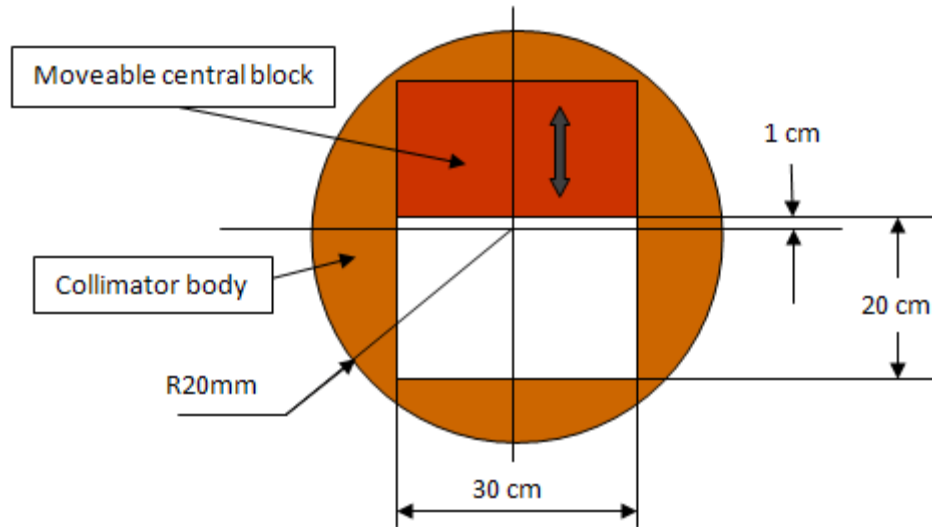


Figure 8.14. Conceptual cross-section of the asymmetric collimator.

The External Muon Beamline Shielding Elements surround the Transport Solenoid and are supported off the building floor as close as possible to the TS cryostat (see Figure 8.15). The primary purpose of the External Muon Beamline Shield is to reduce the flux of neutrons that reach the Detector Solenoid region. The concern is that neutrons could fire the Cosmic Ray Veto or scatter into the sensitive detectors in the Detector Solenoid.

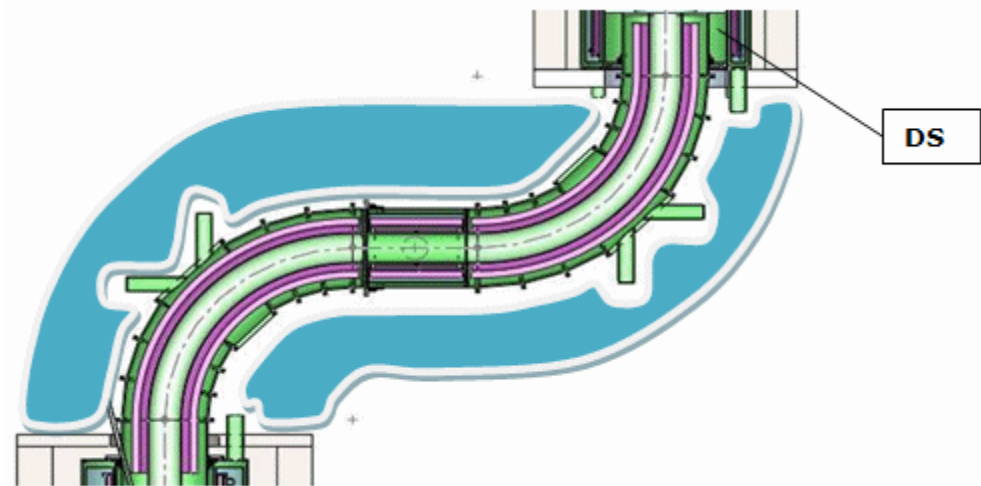


Figure 8.15. Planned area for external Muon Beamline Shielding (blue area).

External Muon Beamline Shielding could be constructed from concrete or polyethylene bricks assembled inside support frames. The geometry of this external shielding will be defined after a neutron background simulation is completed. The position and mass of each of the external shielding components will be defined after a preliminary engineering shielding design is completed. The structural support and

installation fixtures for the External Muon Beamline Shielding will be designed to accommodate the gravity loads of the Shield. Parts of the External Shielding may be manufactured in sections, which will be individually moved into the area around the Transport Solenoid.

Considered Alternatives to the Proposed Design

Since further evolution of the Mu2e Experimental Setup supported by beam studies might reveal a need to introduce Internal Muon Beamline shielding, two alternative solutions, shown in Figure 8.16 and Figure 8.17, have been developed. The first alternative design of the Internal Muon Beamline Shielding is integrated with the design of the Transport Solenoid cryostat vacuum tube (see Figure 8.16). The segmented vacuum tube will have similarly segmented shielding blocks. Shielding blocks will be attached to the inner surface of the vacuum tube for each segment before connecting them to the whole assembly. The Internal Muon Beamline Shielding will be supported by the TS cryostat vacuum tube.

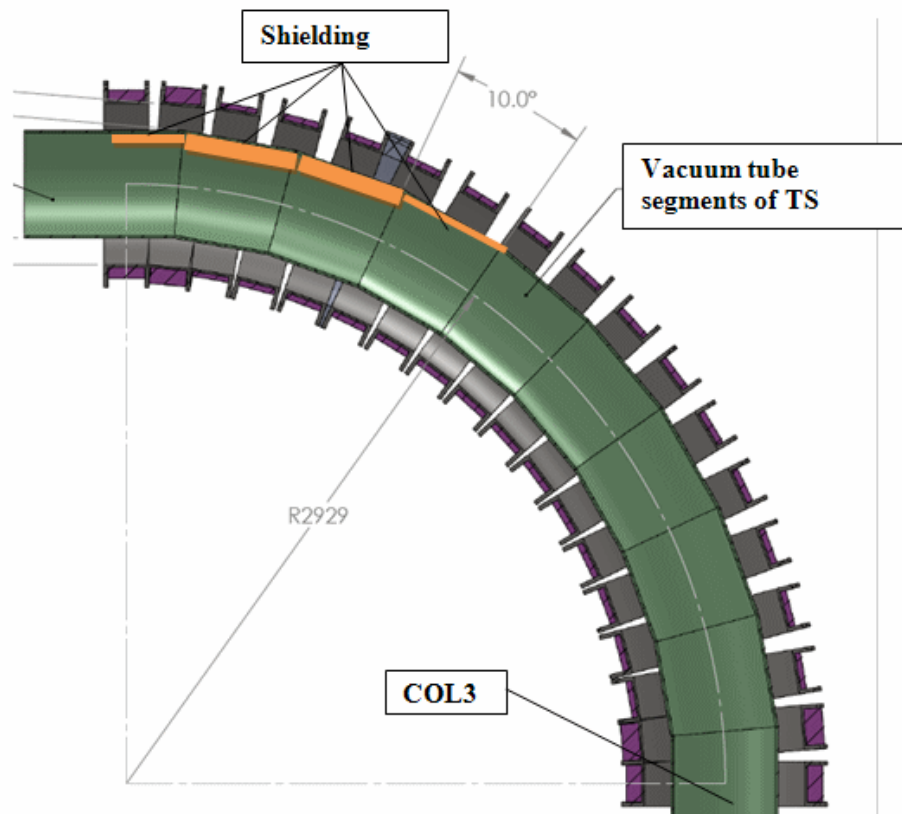


Figure 8.16. Conceptual Design for the Internal Muon Beamline Shielding.

Parts of the Beam Shielding may need to be manufactured in sections, which will be individually installed in the bore of the Transport Solenoid. The beam shielding does not require active cooling or monitoring, thus there are no cooling or electrical interface concerns.

For the second alternative design the Transport Solenoid cryostat vacuum tube is made from two halves and the shield tiles and collimators are installed inside each half tube before final mid-plane welding of the bore assembly. This design might be necessary if a continuous smooth inner surface is required for the cart used to access the Transport Solenoid to map the magnetic field (See Section 7.3.6). The primary disadvantage of this alternative is the high cost of constructing the cryostat in two halves as well as a possibility of tube shape deformation during welding. Installation of this completed tube assembly inside the TS solenoid is challenging as well. The proposed method for this installation is shown in Figure 8.18. Rollers or bearing pads will be used to support the tube assembly.

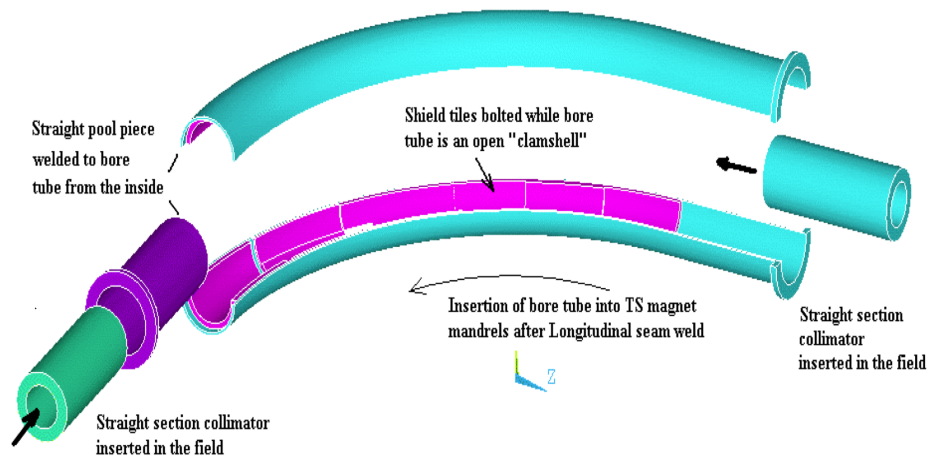


Figure 8.17. Design of the muon beam line shielding from MECO.

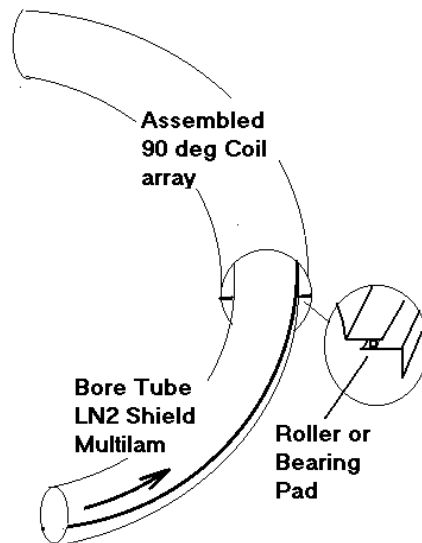


Figure 8.18. Bore tube insertion method from MECO.

8.3.4 Muon Stopping Target

The muon stopping target consists of 17 circular aluminum foils that are arranged coaxially. They are equally spaced 50 mm apart and have a thickness of 0.2 mm. The radii range from 83 mm to 65 mm and are tapered with decreasing radii in the direction of decreasing magnetic field. The position of the target in the Detector Solenoid is such that the first foil is at 1.57 T and the last at 1.30 T.

There are several physics requirements [4] that limit the choice of target material as well as the geometry. The selected material must have a conversion energy that is higher than the maximum photon energy from muon radiative capture ($\mu^- + (A, Z) \rightarrow (A, Z-1) + X + \gamma$), which can induce background. To avoid prompt backgrounds from the beam, data taking begins about 700 ns after the peak of the proton beam pulse. The lifetime of the muon in the target material (which decreases with increasing Z) must be long enough that a significant portion of the muons remain after 700 ns, but short enough that most decay before the next arriving proton pulse at about 1700 ns. However, the expected conversion rate increases with increasing Z , so that it is advantageous to choose a material with high Z . To reach the required sensitivity, at least 40% of the muons must stop in the target. Finally, the target geometry must be chosen to minimize energy loss from potential conversion electrons, minimize background contamination from sources passing through the target (beam electrons, cosmic rays, etc.), maximize the interception with the muon beam, and minimize the rate of DIO electrons that can reach the tracker. A schematic of the proposed design is shown in Figure 8.19.

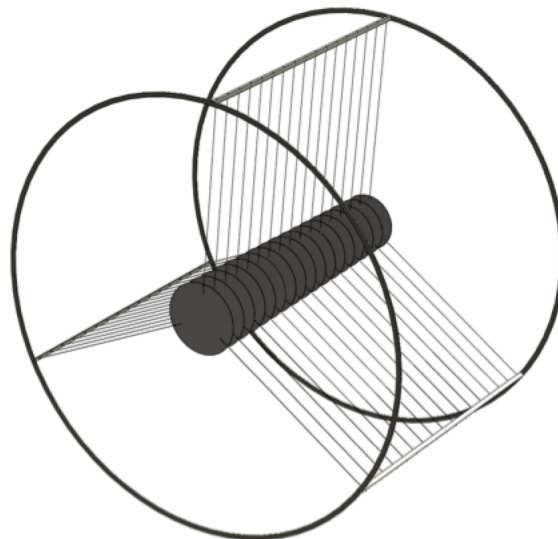


Figure 8.19. Schematic of the stopping target and support.

Stopping Target Material

The stopped muon lifetime and the muon conversion rate as a function of Z are shown in Figure 8.20 and Figure 8.21. Selenium and antimony have the highest conversion rates, but they also have short muon lifetimes. The requirement that the muon radiative capture endpoint energy of the γ be below the conversion energy is equivalent to the condition that the rest energy of the nucleus (A, Z) be below the rest energies of the possible combinations of $(A, Z-1) + X$. For the target materials that also satisfy the other requirements, the differences are 2.5 MeV (aluminum), 600 keV to several MeV (titanium, depending on isotope). However, in the case of titanium it is possible for oxygen to penetrate the foil and contaminate the material. Since oxygen has a lower Z than aluminum the endpoint of the DIO spectrum is higher, so the oxygen contamination can lead to a severe background. Taking these various factors into account, aluminum is chosen as the target material.

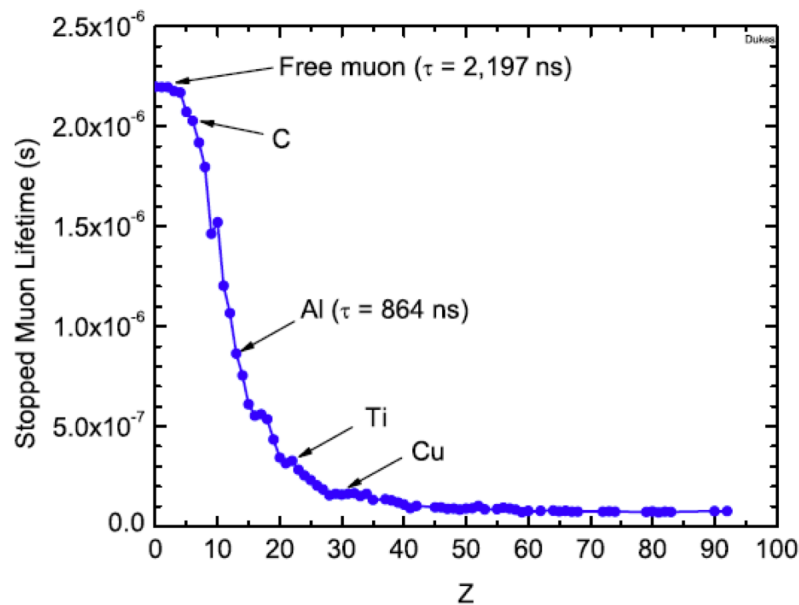


Figure 8.20. The stopped muon lifetime vs. Z .

Position

The graded magnetic field reflects electrons that are emitted in a direction away from the tracker. The position of the target in the field is chosen to be such that the first foil is at 1.57 T and the last at 1.30 T.

Geometry

The geometry of the target must be chosen so that the maximum number of muons are captured while minimizing the energy loss of the conversion electrons. Figure 8.22 shows the conversion electron energy spectrum for a configuration of 8

foils (each 400 microns thick), 33 foils (each 100 microns thick), and 17 foils (each 200 microns thick). The mass of the each target configuration is kept the same. An optimal geometry is found to be 17 foils.

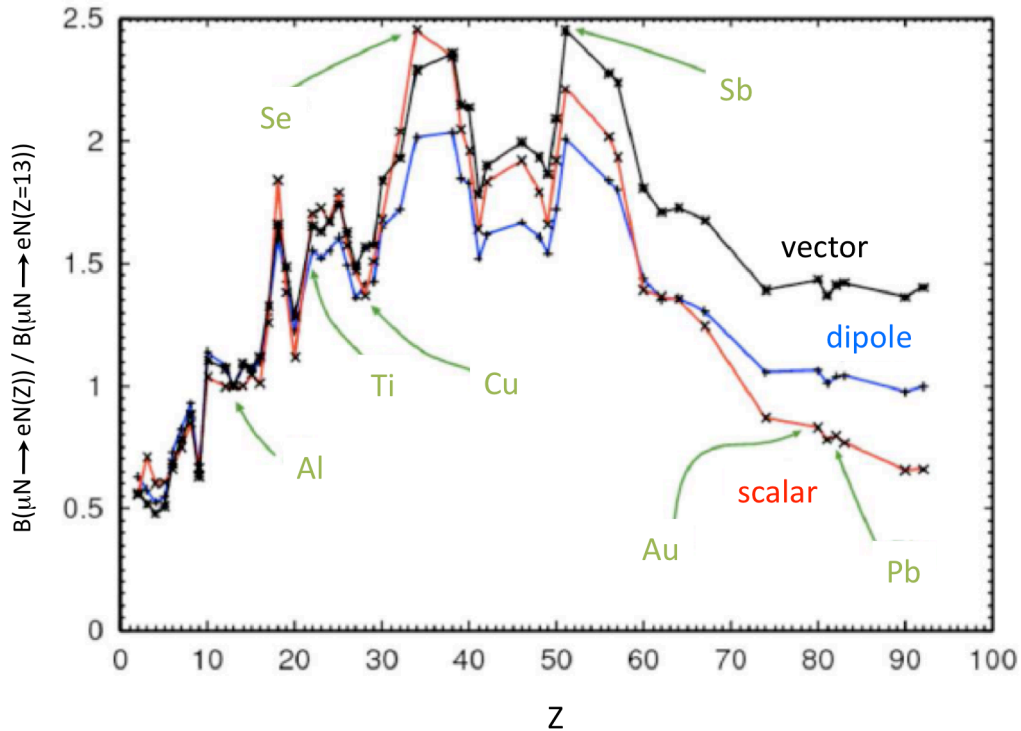


Figure 8.21. The muon conversion rate vs. Z , normalized to the rate in aluminum.

As is stated in the requirements, the target needs to stop at least 40% of the muons exiting the TS to achieve the desired sensitivity. A simulation of the momentum distribution for muons, overlaid with the momentum distribution of stopped muons, that encounter the target is shown in Figure 8.23. According to simulation, approximately 49% of all muons exiting the TS are stopped in the target with the geometry of 17 foils.

The effects of target misalignment (conservatively estimated to be ± 2 mm) would be to increase or decrease the number of DIO electrons striking the tracker. The reconstruction cannot place the origin of the electron to smaller than the spacing between the foils, so that misalignment does not have a significant effect. Misalignment of 2 mm has minimal impact on effort to track muons back from the tracker to the stopping target because the tracking uncertainty is as large or larger.

Support Structure

The support structure holds the stopping target in place in the center of the Detector Solenoid. Because of the diffuse nature of the muon beam as it enters the

Detector Solenoid, a significant number of muons will strike the support structure and produce DIO electrons. Therefore, the support structure must be made of a high Z material because the endpoint of the DIO spectrum and the muon lifetime decreases as Z increases. The chosen material is tungsten.

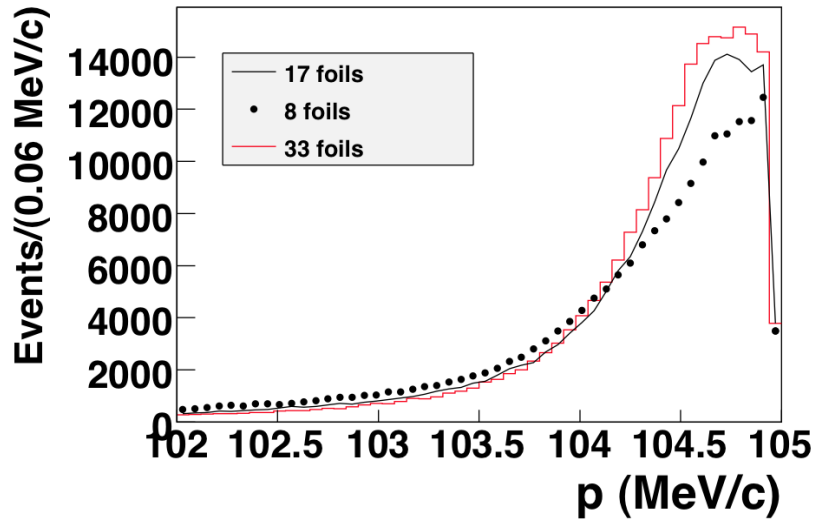


Figure 8.22. The conversion electron momentum spectrum of a target configuration of 17 foils (black line), 8 foils (black dots), and 33 foils (red line). For each target configuration, there are 500k muons that are required to convert to an electron when stopped in the target.

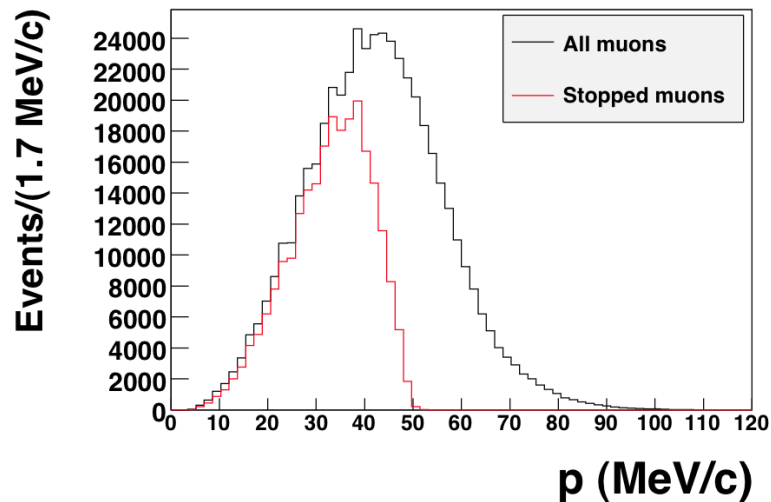


Figure 8.23. The incident muon distribution overlaid with the stopped muon distribution for the geometry of 17 foils. There are approximately 500k incident muons.

Thermal Properties

Beam electrons and muons deposit about 400 mW of heat in the muon stopping target. The heat must be dissipated through a combination of radiation and

conductive heat transfer through the support structure. Taking into account the surface properties of aluminum, Ref [3] indicates that radiation alone is sufficient to dissipate the heat and keep the target temperature near 60° C.

Considered Alternatives to the Proposed Design

Some studies of a helical stopping target configuration have been done, with the goal of increasing the muon stopping rate but reducing the amount of material traverse by conversion electrons. The geometry was found to be helpful for these issues, but the drawback is that it is not optimal for positive particles. One of the main calibrations for the experiment uses positive pions that are stopped in the target. The positrons that result from the two-body decay provide an energy calibration. There are also plans to study alternative geometries where each target disk is replaced with a conical shaped element. From geometric considerations, incoming muons would see more material, increasing the stopping rate, while conversion electrons in the acceptance of the tracker would see less target material, improving the momentum resolution function. If additional studies indicate that these geometries are more favorable than the current design, it will be adopted.

8.3.5 Stopping Target Monitor

Muons come to rest in the stopping target and almost immediately emit X-rays, which signal the formation of muonic atoms. The estimated muon stopping rate is few times 10^{10} Hz. From aluminum, these X-rays are in the range of 66 keV to 446 keV. Oxygen, which can be an impurity in the target foils, has a characteristic x-ray at 134 keV ($2p \rightarrow 1s$). In order to study these X-rays, a germanium detector (shown in Figure 8.24) will be utilized, which can detect photons with an energy of a few 100 keV to ~ 1 MeV with sufficient photopeak efficiency and energy resolution.

There are several requirements [5] that determine how the germanium detector should be placed. Sufficient collimation should be provided so that the detector only views the target. Additionally, the rate of the X-rays at the crystal must be compatible with the detector's capability. The detector should be placed far from the target because of the high X-ray rate. The material between the target and the detector (collimators, windows) should emit muonic X-rays that do not fall too close to the X-rays from aluminum. This material should also not absorb X-rays from the target. Finally, the detector must lie outside the enclosed Detector Solenoid so it can be serviced periodically to repair the damage from incident neutrons.

A significant background to the muonic X-rays is bremsstrahlung photons coming from electrons that intercept the target. This background should be kept to a minimum to reduce the flux of photons arriving at the germanium detector. Most electrons

arrive about 100 ns before the muons, therefore the germanium detector must recover in this short time period from the effects of the electron flush.

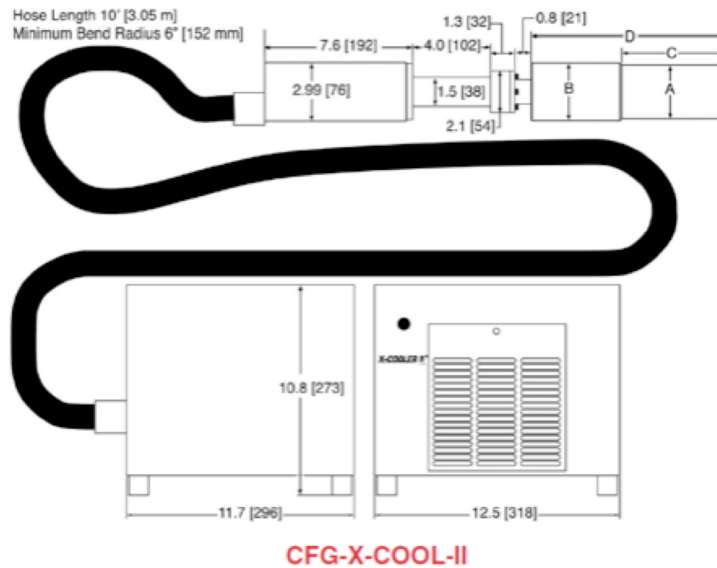


Figure 8.24. Configuration of ORTEC GMX HPGE detector fitted with X-cooler system.

Surrounding Material

X-ray collimation will be provided by a pipe inserted into the steel and concrete shielding downstream of the detector Solenoid. A window will separate the vacuum of the Detector Solenoid from the entrance of the collimation pipe. From these materials, the muonic X-rays have an energy that is well separated from the characteristic X-ray spectrum from aluminum.

Radiation Damage

Neutrons, coming from sources such as muon capture, will damage the germanium detector. Once the efficiency loss from radiation damage reaches unacceptable levels the detector has to be removed and annealed. According to the ORTEC catalog, a neutron fluence of 10^9 is will degrade the detector efficiency to less than 70%. It is estimated that annealing will be required every couple of months. The plan is to have two germanium detectors so that there is no down time associated with the annealing process.

Cooling

Germanium detectors operate at liquid nitrogen temperature. A commercially available mechanical cooler, such as the X-cooler system from ORTEC Inc., will be used.

Considered Alternatives to the Proposed Design

In the event that radiation levels from neutrons and Bremstrahlung photons are too high to operate a germanium detector, an alternative mode of operation is possible. The germanium detector could be used to benchmark the rate of muon captures to rates in detector elements at reduced proton beam intensities. The germanium detector can be removed during production running at full intensity to avoid damage and properly scaled detector rates can be used to estimate the number of captured muons. The germanium detector can be remounted periodically as a cross check.

8.3.6 Proton Absorber

The proton absorber (shown in Figure 8.25) made of polyethylene, is a tapered cylindrical shell 0.5 mm thick with a radius slightly smaller than the inner radius of the tracker. The proton absorber is 210 cm in length and extends from the end of the stopping target to the beginning of the tracker. The physics requirements [6], that constrain the design of the proton absorber mandate that it should reduce the rate of protons at the tracker to allow proper reconstruction of electron tracks while minimizing the energy loss and straggling of conversion electrons that intercept it. Additional rate in the tracker can result in reconstruction errors that add a tail to the momentum resolution function and creates background. Energy loss and straggling in the proton absorber can also add tails to the resolution function. The proton absorber must be designed to balance these two effects. The proton absorber should not intercept the muon beam.

Material

To minimize the impact on the momentum resolution function for conversion electrons the proton absorber should be constructed from a low Z material. This is satisfied by the choice of polyethylene. HDPE is the initial choice pending simulations, because it represents an acceptable balance between ease of construction and density.

Support Structure

Since the support structure of the proton absorber lies well outside the extent of the muon beam, it is not constrained by the same requirements as the support structure for the stopping target. However, the wires that connect the proton absorber to the target frame are also made of tungsten. Figure 8.25 shows the space frame that supports the target and proton absorber. It will be constructed from stainless steel and will be mounted to the rail system internal to the Detector Solenoid. Figure 8.26 shows a detail of the connection between the space frame and the rail system bearing block.

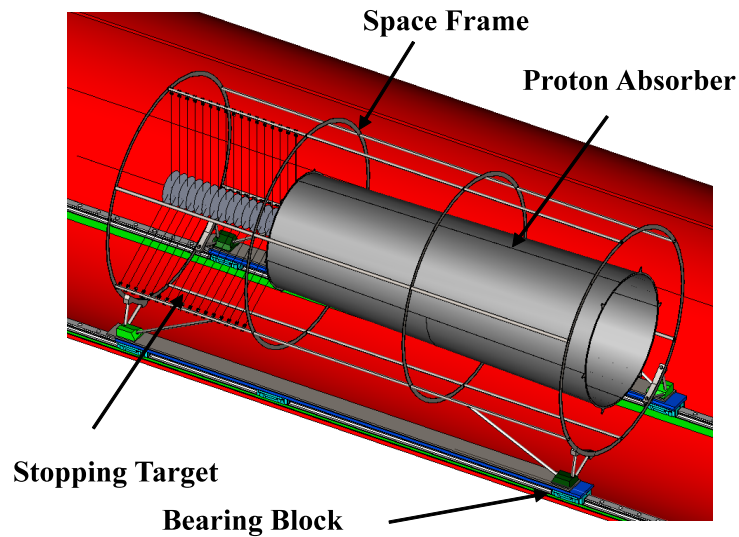


Figure 8.25. The proton absorber, stopping target and stainless steel space frame that supports the target and proton absorber.

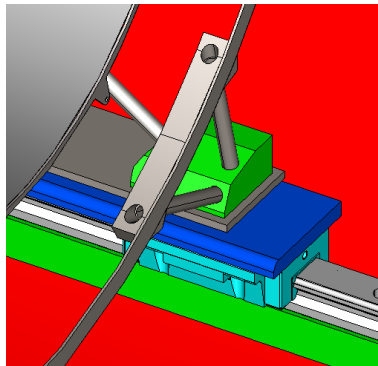


Figure 8.26. Detail of the connection between the space frame and the internal rail system.

Considered Alternatives to the Proposed Design

Thin polyethylene sheet is rather difficult to support. A prototyping effort is under way to evaluate this concern. Alternate low Z materials with better mechanical properties exist (other hydrocarbon polymers or Styrofoam) and will be studied if necessary.

The nominal shape of the proton absorber is a simple hollow cone. Other shapes, such as the “blade” configuration shown in Figure 8.27, are being considered. The blade alternative would allow conversion electrons to spiral through unaffected while still intercepting most protons. Simulations will determine which configuration is preferable.

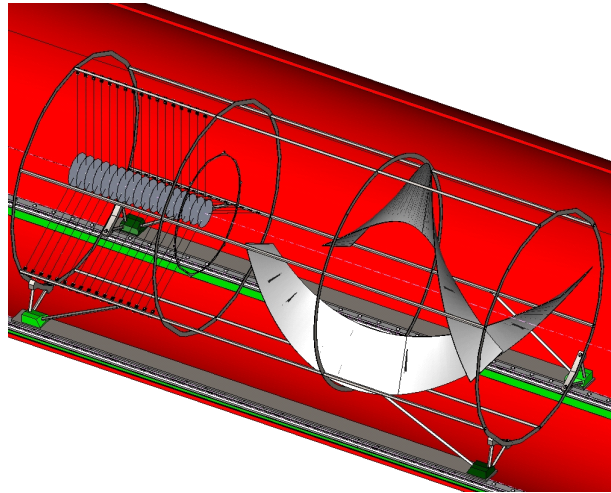


Figure 8.27. Alternate spiral “blade” configuration of the proton absorber.

8.3.7 Muon Beam Stop

The purpose of the Muon Beam Stop (MBS) is to absorb the energy of beam particles that reach the downstream end of the Detector Solenoid to minimize the rate of accidental particles in the active detectors from muon decays and captures in the Beam Stop. The Muon Beam Stop is located within the warm bore of the Detector Solenoid, downstream of the calorimeter. It is supported and aligned by the rail system internal to the Detector Solenoid and moves into place on ball bearing blocks. A pictorial view of the muon beam stop is shown in Figure 8.28.

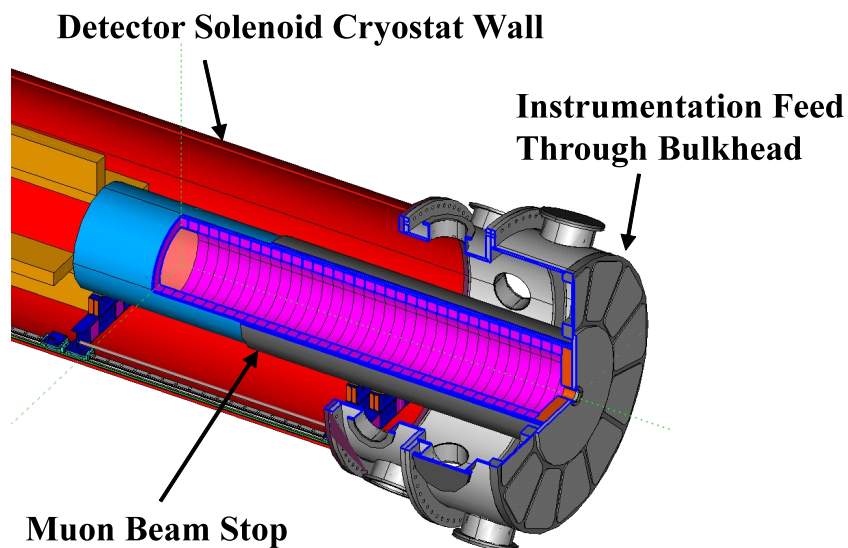


Figure 8.28. Muon Beam Stop in position.

The Muon Beam Stop consists of several cylinders, composed of different materials. Components consisting of stainless steel, lead and high density

polyethylene (HDPE) will be assembled and bonded together. The HDPE may be doped with either boron or lithium. Figure 8.29 shows the beam stop with the individual component names and materials labeled.

The end plug (labeled CLV2 in Figure 8.29) contains a 10 cm diameter hole through the center to provide a line-of-sight for the Muon Stopping Rate Monitor located on the muon beam axis downstream of the MBS. The precise sizes, volumes and masses of the Muon Beam Stop components are described in [7]. Volumes and diameters of each component are derived from simulations.

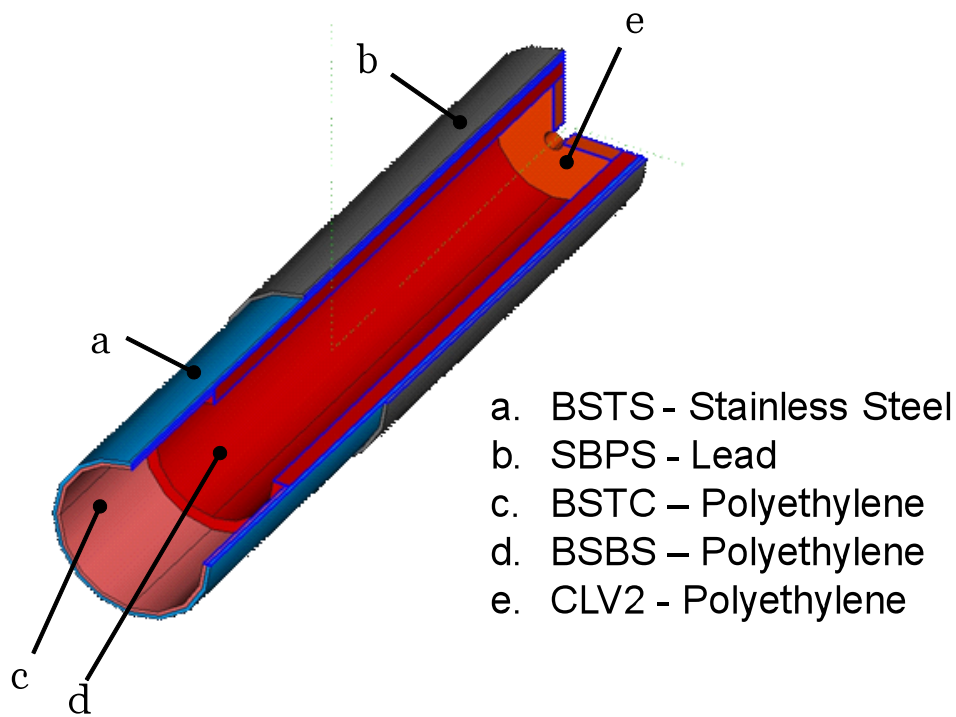


Figure 8.29. Muon Beam Stop components.

Manufacturing and Assembly

The Muon Beam Stop will be manufactured and assembled in outside facilities and transported as an assembly to the experiment hall. The stainless steel outer shell will consist of a single piece that is rolled and welded. The polyethylene pieces will be made of a series of rings, separately machined and bonded together with no line-of-sight cracks, except for CLV2, which will be made from a single sheet. The thickness of the rings will be limited to 100 mm, the manufacturing limits on the raw material. A drawing of an individual ring is shown in Figure 8.30.

The Muon Beam Stop will be made in several steps. First, the stainless steel tube will be manufactured and shipped to Fermilab for inspection. Measurements of the inside diameter of the tube will be used to determine the precise outside diameter of

the HDPE parts that will fit inside it. The stainless tube will then be sent to a lead vendor, where the lead tube will be rolled and welded around the existing stainless tube. Finally, the stainless/lead tube will be shipped to Fermilab for assembly with the HDPE parts.

Support and Alignment

The Muon Beam Stop will be transported into position, supported and aligned by a linear rail system and bearings, manufactured to fit inside the Detector Solenoid warm bore and to support the full mass of the beam stop. The Beam Stop will rest on and be aligned to the linear rail system using a support structure that contacts the linear bearings at four positions as shown in Figure 8.31.

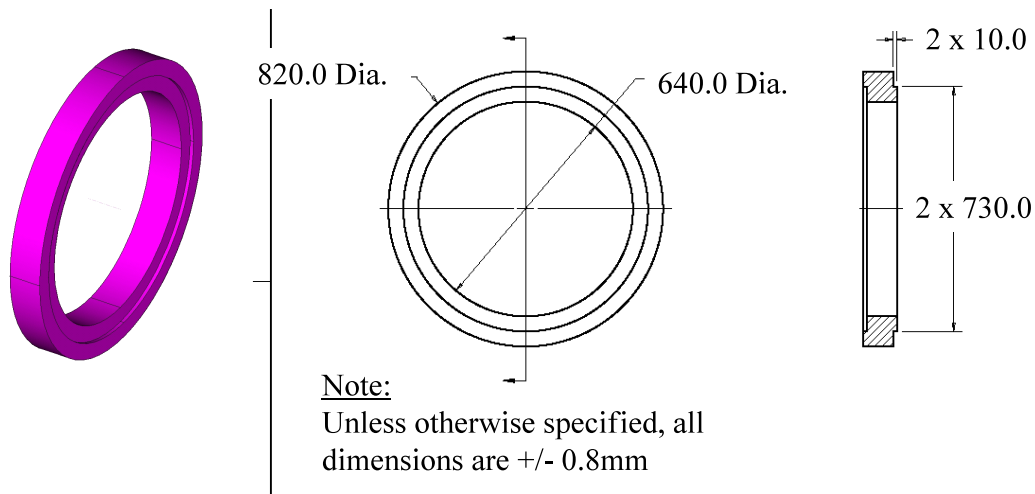


Figure 8.30. Muon Beam Stop in final position with internal support structure.

The Muon Beam Stop will be rolled into position while connected axially to the Tracker, Calorimeter and Instrumentation Feed Through Bulkhead (IFB). This is necessary because the cables and cooling tubes from the Tracker and Calorimeter are terminated at and permanently attached to the IFB. Although connected in the axial direction, these components will be aligned separately in x and y. The support positions and installation procedure for the MBS are given in [9]. The MBS will be aligned with respect to the center of the Detector Solenoid magnetic field as described in [10].

Considered Alternatives to the Proposed Design

The Muon Beam Stop component sizes and materials have been chosen based on a series of design studies, simulations and manufacturing considerations. Further study may call for some modification in the size and shape of the rings. Proposals to alter the length and/or diameter of the MBS are under consideration [13].

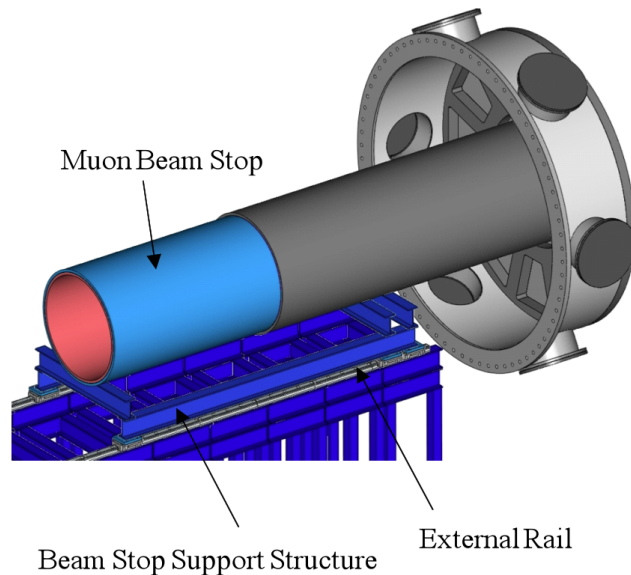


Figure 8.31. Muon Beam Stop in final position with internal support structure.

Although the baseline material of the polyethylene parts is HDPE, several types of doping are being considered. Boron doping between 5% and 30%, lithium doping of 7.5% natural lithium (92.6% lithium-7 and 7.4% lithium-6), or enriched lithium, with higher percentages of lithium-6, may be used for all or part of the polyethylene parts.

In the baseline design, the MBS is completely supported by the rail system. Partial support from the cryostat wall, by attachment to the IFB on the downstream end, is being considered. This would allow the rear bearing blocks to bear less weight and possibly improve the mechanical stability of the MBS, but would result in a more complicated support system. This alternative may be necessary if the length of the MBS is increased.

8.3.8 Neutron Absorbers

Absorbers must be placed around the Detector Solenoid to limit the number of neutrons reaching the Cosmic Ray Veto. These absorbers surround the DS vacuum enclosure and will be supported independently from the Detector Solenoid.

The Absorbers are constructed primarily of concrete blocks. The blocks include magnetic steel reinforcement bars and brackets. Analysis will need to determine whether the incorporation of the steel parts so close to the DS solenoid field will be acceptable. An illustration of a “typical” concrete block is shown in Figure 8.32. A specification for the composition of the concrete and steel to be used is given in [8].

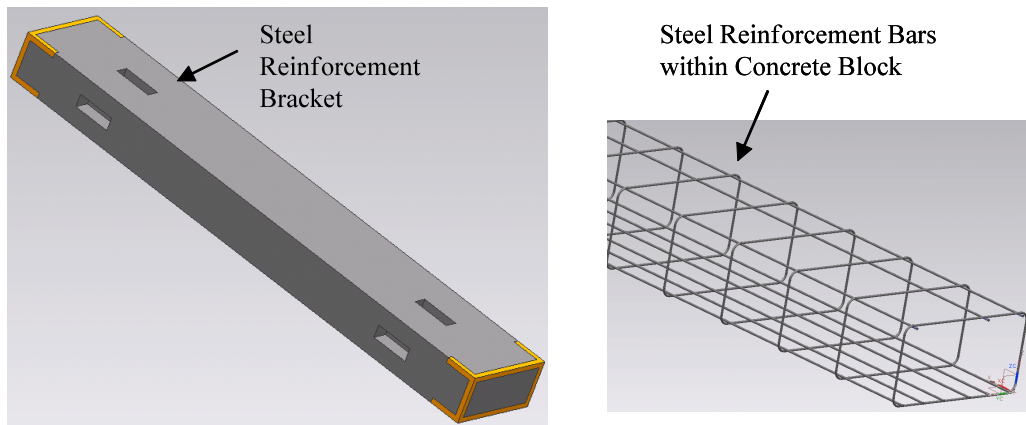


Figure 8.32. Neutron Absorbers and Shielding.

The neutron absorbers are made of two different sections. They are shown assembled in Figure 8.31. The central section encompasses the entire DS and a section of the VPSP. This section occupies the axial space that was formerly taken by the cryostat iron. The end cap shielding encloses the IFB and the termination of the connectors for the cables and pipes from the Tracker and Calorimeter.

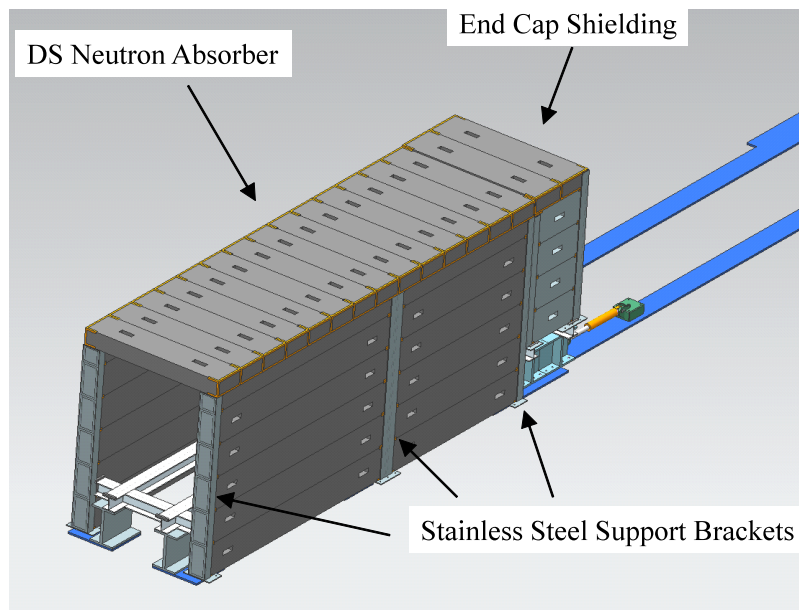


Figure 8.33. Overall view of Neutron Absorbers and Shielding.

Manufacturing and Assembly

Due to manufacturing constraints and to facilitate installation, the absorbers and shielding are made of many pieces. Figure 8.34 and Figure 8.35 show in more detail how the central section and the end cap shielding are constructed. These components will be assembled from many concrete blocks of different sizes. The stacks of

concrete blocks are supported by stainless steel brackets which provide structural support and make assembly easier. An opening in the bottom of the end cap shielding allows an exit area for cable and cooling tubes from the Tracker and Calorimeter.

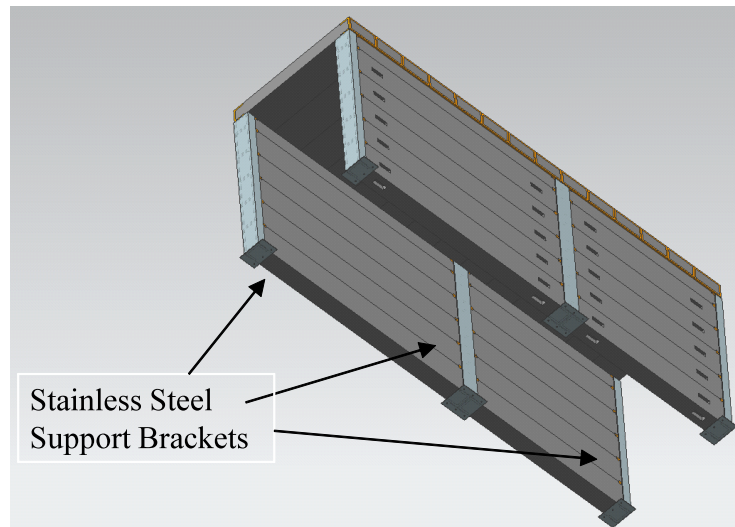


Figure 8.34. Bottom view of Central Section of the Neutron Absorber.

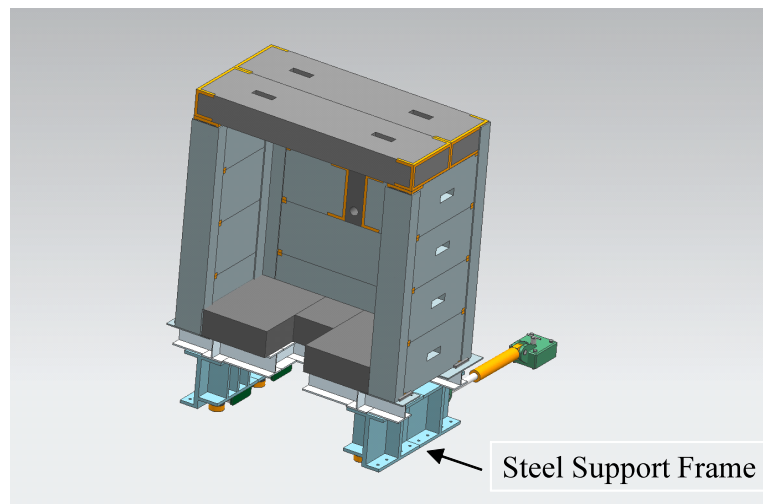


Figure 8.35. End Cap Shielding.

Support and Alignment

The concrete blocks that compose the central absorber and end cap shielding will be generally self-supporting. Both sections will be built in the detector building using the available overhead crane. The central area will rest upon the floor of the detector building, while the end cap shielding will be supported by a steel frame as shown in Figure 8.35. As noted above, some stainless steel brackets will be necessary to

facilitate support. Structural analysis to determine the size and frequency of supports is taking place.

The absorbers will be aligned with respect to the center of the Detector Solenoid magnetic field using fiducials mounted to the exterior of the DS cryostat [10]. The concrete end cap shielding will be rolled into position on a track containing Hillman rollers and supported by pads that will be shimmed to the correct height. It can then be rolled back to allow access if necessary for maintenance.

Considered Alternatives to the Proposed Design

Although the concrete blocks contain magnetic steel reinforcement bars and brackets, austenitic stainless steel (304 or 316) could be substituted if the magnetic steel is found to be unacceptable. Additional cost would be incurred for the manufacture of blocks with stainless steel. Ongoing studies will determine whether stainless steel is necessary for this application, and the added cost.

It is possible to design the end cap shielding to rest on the floor of the detector hall, as does the central section. This may be slightly cheaper to build, and will not require a frame or hydraulic equipment to allow axial movement. However, this alternative would require that the structure be disassembled with the overhead crane to allow access to the DS internal area. This would in turn require disassembly of the ceiling of the detector hall.

Water is a good absorber of neutrons and could be used if an additional external absorber is desired. A water tank can be built with walls of HDPE. Such a tank could surround the DS vacuum space between the outside wall of the cryostat and the concrete enclosure. A conceptual design of the tank is shown in Figure 8.36.

If an absorber is desired within the vacuum space of the DS cryostat, HDPE tanks could be built for this application. If used internally, water is not desirable because, although the possibility of a leak is very small, any risk of a water leak in this area is unacceptable. Internal tanks could be filled with a powder containing boron or lithium to eliminate this possibility.

8.3.9 Detector Support Structure

The detector support and installation system will be used to transport and align components within the Detector Solenoid. The muon stopping target, proton absorber, tracker, calorimeter, and muon beam stop will be moved accurately and safely into position and aligned with respect to the standard Mu2e coordinate system [9]. The components vary significantly in mass (from less than 3 kg to over 4000 kg) as well

as in their alignment accuracy requirements. These components will be supported by the inside wall of the Detector Solenoid cryostat.

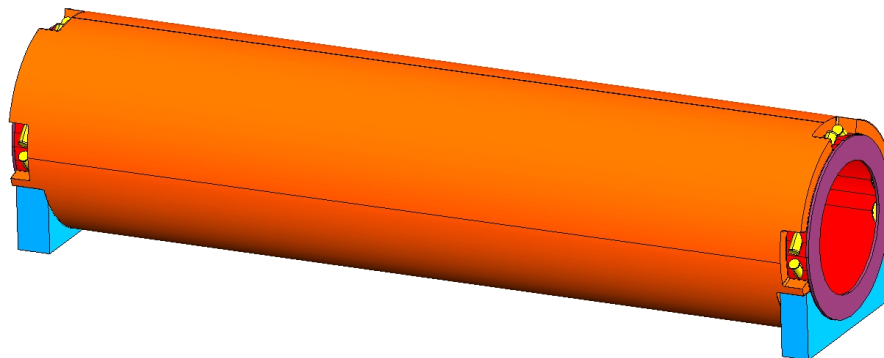


Figure 8.36. Water tank (shown in orange) surrounding the DS cryostat.

An overall view of the detector support and installation system is shown in Figure 8.37. The components are supported by two rails and transported by linear ball bearing blocks. Two separate rail systems will be implemented, the “internal” and “external” systems. Once transported, the alignment of all components will be maintained by the internal rail system. In Figure 8.37, the muon stopping target and proton absorber are shown in their final positions, while the remaining components are still located on the external rail system.

The internal system is shown in cross section in Figure 8.38. It will be imbedded into the internal neutron absorber and attached to stainless supports that are welded onto the inside wall of the DS cryostat, also shown in Figure 8.38. It will support the weight of each component, allowing all alignment criteria to be achieved. The alignment criteria for each component are given in [9]. In the proposed design, the rails and blocks are made exclusively of non-magnetic components. Areas of the neutron absorber are cut away to provide clearance for the rails in a way that minimizes any line-of-sight cracks.

The external rail system (Figure 8.37) is located outside of the Detector Solenoid and is used to transport components into position inside the DS warm bore. It consists of a series of stands, each of which can be installed or removed as needed. The external stands are made of structural steel, each with sections of rails mounted to the top surface that can be connected and disconnected accurately. The rails will be identical to those used for the internal system, and the last stand, closest to the cryostat, will be attached to the internal system during installation.

Figure 8.39 and Figure 8.40 show a single external stand with the rail system attached, and the connection between the final external stand and the internal system, respectively.

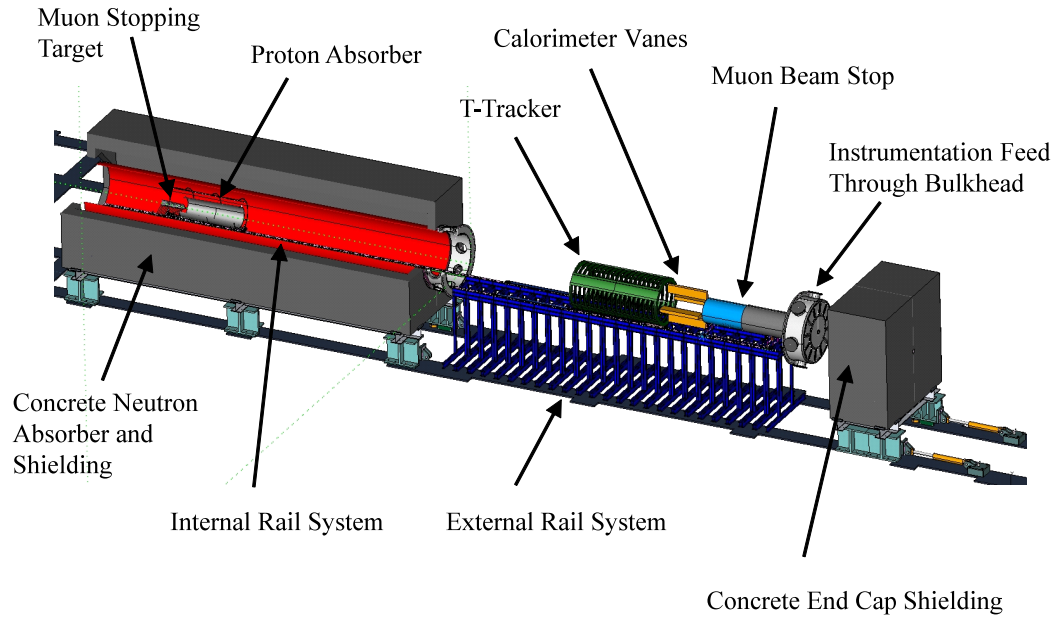


Figure 8.37. Conceptual Design of the Rail System.

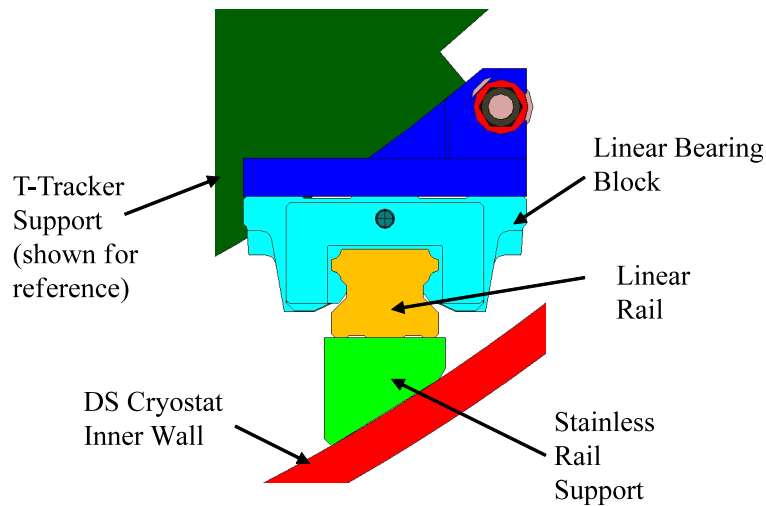


Figure 8.38. Cross Section of the Internal Rail System.

Each component will be aligned to the Detector Solenoid warm bore and attached to the rail system separately. Each will include support elements that provide the necessary structural support. Four leveling feet will allow for alignment of each component. The leveling feet will contact the linear bearing blocks. The specific

position of each bearing block has been determined from a structural analysis described in [9]. Descriptions of the support structures are included in the conceptual design sections for each component.

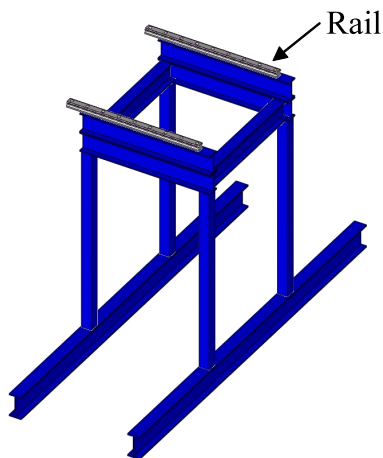


Figure 8.39. Individual external rail system Stand.

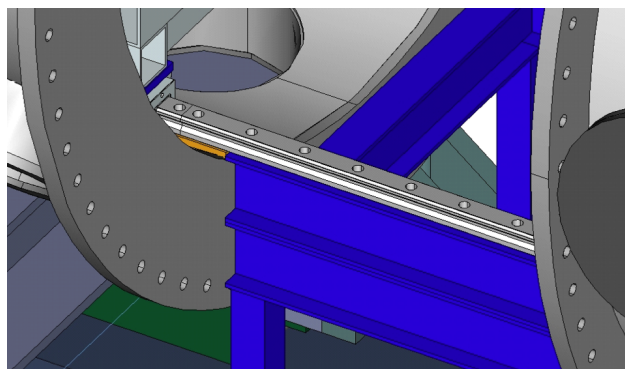


Figure 8.40. External to Internal rail system Attachment.

Cabling and cooling tubes from the tracker and calorimeter will be installed and attached to the Instrumentation Feed-Through Bulkhead (IFB) before moving the entire assembly, including the detector components, into position [9]. The cables and tubes will pass over the Muon Beam Stop before being terminated in the IFB. This mandates that the tracker, the calorimeter, the beam stop and the IFB be rigidly attached to one another and moved into place as a single unit. After being individually aligned, these components will be connected axially by attaching their respective bearing blocks, as shown in Figure 8.41. Figure 8.37 shows these components in their positions before being rolled into the Detector Solenoid bore.

Manufacturing and Assembly

Several manufacturers have been identified who make rail systems that will potentially fit the requirements of the project with respect to accuracy, load and

magnetic properties. The proposed design has been developed in conjunction with THK Co., LTD.

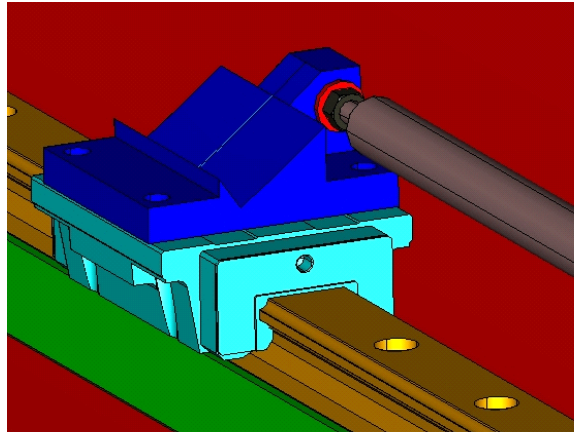


Figure 8.41. Axial Component Attachment System.

The supports for the internal rail system will be welded to the inside wall of the Detector Solenoid by the cryostat manufacturer before the DS coil is wound. The rail system and bearing blocks will be manufactured and tested outside Fermilab by the rail system vendor. Individual parts will be inspected upon their arrival. The parts will then be mounted by Fermilab personnel to the existing supports, aligned and shimmed into position with respect to the center of the DS magnetic field. The components of the internal and external rail systems will be identical in cross section.

Detector Solenoid Component Installation Procedure

The components to be installed by the system described in this section are the muon stopping target, proton absorber, tracker, calorimeter, and the muon beam stop. The Instrumentation Feed-Through Bulkhead and end cap shielding will be moved on a different rail system, discussed elsewhere, although the IFB is required to be connected axially to the other components. The assembly procedure for installation of components is described in [9].

Considered Alternatives to the Proposed Design

A rail system using Teflon guides instead of nitride linear ball bearing blocks has been considered. Such a system would be equally non-magnetic, but not as accurate, and involve a much higher coefficient of friction that requires more complicated methods of moving the heavy objects.

A similar rail system comprised of magnetic components that would have to be removed after installation has been evaluated. Systems such as these are more readily available at lower cost, have an equally low coefficient of friction and are just as

accurate. However, the requirement to remove the rail system prior to operation would make it necessary to place the components on a separate set of fixed supports before removing the rails. This would make the procedure for installation and alignment, as well as removal and replacement of components, significantly more complex.

Bolting the rails to the walls of the cryostat has been evaluated as an alternative to welding. This would eliminate any possibility of distortion to the inner wall from welding as well as eliminate any risk of increased magnetic permeability after welding. However, the difficulty of placing the holes accurately, as well as structural issues related to the wall thickness of the tube, make this solution less desirable. It is still a possibility if tests reveal that the amount of magnetic permeability created by welding is unacceptable.

Instead of extending the rail system to the upstream end of the cryostat, the rails could terminate at the downstream end of proton absorber. In this case, the muon stopping target and proton absorber would be mounted to fixed supports directly attached to the DS cryostat wall. This alternative has the advantage of having a slightly lower cost, due to the shorter length required for the rails and the elimination of a few bearing blocks. However, it has several disadvantages. The magnet measurement system would not be able to extend to the upstream end of the DS. Also, the movement of the stopping target and proton absorber into the bore would become more difficult. They would either need to be transported by hand or cantilevered from the rail system before being set on the fixed supports. In either case, it would be more difficult to align the components with multiple “iterative” adjustments, because the alignment adjustments would have to be done in place, rather than outside the bore area. Replacement or realignment, if necessary, would also be more difficult.

8.3.10 System Integration, Tests and Analysis

The Muon Beamline is a WBS Level 2 subproject that consists of many different deliverables. The Muon Beamline subproject is divided into ten Level 3 deliverables. The integration task has been developed to manage the relationship of the deliverables with one another and with systems in other Level 2 subprojects, recognizing that proper integration requires effort, resources and manpower.

Alignment is another task that spans deliverables and subprojects so it is necessary to have an integrated, global approach across the entire Muon Beamline subproject. System tests and global failure mode analysis are also generalized tasks

that require integration across the entire subproject. A detailed description of the System Integration, Tests and Analysis is described in [10].

8.4 Risks

The Muon Beamline deliverables, design and construction (L3) sub-projects of the Muon Beamline sub-project are well within the experience and expertise of the technical staff and physicists who are participating. Every effort has been made to specify these (L3) sub-projects in a manner that reduces the risk to an acceptably low level.

The risks identified in the Muon Beamline are summarized in the Mu2e Risk Registry [11]. The greatest identified risk is to the vacuum system if gas loads due to detector material, especially the tracker components that can be subject to strong outgassing and gas permeation through the thin wall of the individual straws, are higher than anticipated.

This risk, before mitigation, has a significant probability to occur. This is considered primarily as a technical risk. If the gas load exceeds 10^{-3} Torr the High Voltage interlock system prevents power from being delivered to the tracker. This could also impact the Project cost and schedule. Mitigation of this risk includes building in extra contingency in the pumping capacity of the vacuum system, strict specifications for gas loads, a program of outgassing tests for materials inside the vacuum and determination of the permeation properties of the straw tube material.

A second significant risk is that a vacuum window is damaged or breaks when the system is evacuated. Physics concerns often demand that vacuum windows be as thin as possible, making it more likely that a break might occur. Should a vacuum window break it could result in harm to nearby individuals, damage to equipment and the spread of radioactive materials. This risk will be mitigated by understanding the physics and technical requirements of each window and designing them to be no thinner than necessary. Operational and administrative controls will also be in place to limit access and activity in the vicinity of vacuum windows when the system is evacuated.

8.5 Quality Assurance

The Muon Beamline sub-project has developed a quality assurance plan [12]. In this section, as an example, the application of the quality assurance plan to the design, procurement and installation of the Muon Beam Stop is described.

- The Muon Beam Stop (MBS) consists of several parts made of three different materials: stainless steel, lead and high-density polyethylene (HDPE). The stainless steel and lead tubes will be designed per ASTM specifications (ASTM A240 and ASTM B749, respectively) and all design procedures will conform to the Fermilab Engineering Policy Manual.
- Engineering drawings for each individual component, sub-assemblies and assemblies will be completed. Tolerances are specified on each drawing in accordance with the Requirements and Specifications (R&S) document. The Fermilab Technical Division Design and Drafting Department will make the drawings, and formally check them according to applicable geometric tolerance standards.
- The drawings will be released to the Technical Division Quality and Materials (Q&M) Department. They will be sent to several outside manufacturers who have been approved by Q&M personnel. After quotations are received, they will be reviewed by personnel from the Fermilab Engineering and Q&M department, and a manufacturer will be chosen.
- The stainless steel tube will be manufactured first. After completion, they will be inspected by the Technical Division Inspection Department, and a formal inspection report will be electronically generated.
- If the tube passes inspection, it will be shipped to the vendor to have the lead tube rolled and welded around it.
- The HDPE parts that fit inside the stainless tube will not be manufactured until the stainless tube has been inspected. The actual manufactured dimensions from the stainless tube will be used to apply the specific tolerances and dimensions to the HDPE. The HDPE rings may need to be made of several pieces and fit together at assembly, due to size limitations from manufacturers.
- The stainless steel/lead tube assembly and the HDPE parts will be manufactured, inspected and approved or rejected by the same process as has been previously described for the stainless steel tube.
- Once all the parts have been received and approved, they will be assembled in an assigned area within Technical Division to ensure that all parts fit and that any required shimming has been established and documented. Cleanliness issues during assembly will be followed according to section 6.2 of the Muon Beam Stop R&S document [7].
- A prototype assembly of the rail system to be used in the Detector Solenoid bore will also be assembled in TD. The assembled Muon Beam Stop will be mounted to this system to ensure that all alignment issues are completely understood.

- A controlled document, or “production report”, will be written during the pre-assembly and alignment, and placed into the Fermilab Engineering Data Management System. Reports of these steps will be included in the general review process of the Muon Beamline sub-projects.
- Finally, the Muon Beam Stop Assembly will be shipped to the Mu2e experimental hall to be installed. During pre-assembly, decisions will be made regarding whether the Beam Stop will need to be partially or fully disassembled for shipment, or whether it can be shipped to the experimental hall as a complete assembly.
- Installation in the experimental hall will be done according to the steps outlined in sections 4.3 and 6 of the Detector Support and Installation System R&S document [9]. Alignment will be done in accordance with Appendix A of the same document.

8.6 Value Management

Value Management is defined as an organized effort directed at analyzing the functions of systems, equipment, facilities, services, and supplies for the purpose of achieving the essential functions at the lowest life-cycle cost consistent with required performance, quality, reliability and safety. Application of Value Management principles to the Muon Beamline sub-project includes physics and engineering studies and project and subsystem reviews to address technical, cost and schedule issues. Value Engineering has been applied in preparing the conceptual design for the Muon Beamline and will continue to be applied throughout the life of the Project.

The Mu2e Project has implemented an internal design review system where each subproject is closely examined to obtain optimal value for the system, given the technical requirements and schedule constraints imposed on it. These reviews are documented in the project’s document database. Documentation and updates are available to the project management staff, subsystem managers and other project personnel.

Value Management is applied for each WBS element at Level 3 or lower (except for WBS 5.1, Project Management). The following items provide a snapshot of Value Management considerations.

Vacuum System

A careful estimate of the vacuum load and selection of materials with known levels of out-gassing will help to properly specify the vacuum system components needed to meet the requirements with an appropriate level of performance margin. Less performance margin is necessary if the loads are well understood. Selection of

materials with low out-gassing rates would reduce the load on the system and might also result in cost savings.

The conductance through the various system components (ducts, ports, etc.) will be studied in detail as part of the optimization of the vacuum pumps.

Collimators

Various drive mechanisms could be used to rotate the collimators in the TSu and TSd straight sections. The available options will be evaluated for cost and reliability.

Muon Beamline Shielding

The External Muon Beamline shielding material around the Transport Solenoid must be optimized to effectively shield the detectors while allowing access to the Antiproton Stopping Window Module region for repairs. The Internal Muon Beamline shielding assembly procedure must be optimized.

Stopping Target

Stopping target tolerances could drive the design and production costs. A careful simulation is required to determine appropriate tolerances that don't compromise performance.

Stopping Target Monitor

Utilizing existing detector solutions for the stopping target monitor should minimize the cost.

Proton Absorber

Styrofoam will be analyzed as an alternative approach to Polyethylene for the proton absorber. This would simplify the mechanical support since Styrofoam is largely self-supporting across the required span, while the required thickness of Polyethylene may not be.

Muon Beam Stop

Simulations of the Muon Beam Stop will be performed to optimize the material dimensions and locations.

Neutron Absorbers

The installation of the neutron absorbers is a complicated procedure due to the number of pieces, their size and shape. The installation procedure still requires optimization to reduce the necessary time and effort.

An attempt will be made to use cheaper, magnetic reinforcement bars in the concrete blocks that surround the solenoid rather than stainless steel. Studies will determine whether this is possible.

Detector Support Structure

The Detector Support Structure will be optimized through close coordination and integration with the components that it must transport and support. Prototypes will be built prior to procurement of final parts to verify performance.

8.7 ES&H

There are several potential hazards associated with the Muon Beamline component fabrication, installation and operation. These hazards are well understood, being similar in nature to other hazards frequently encountered by Fermilab Technical Division personnel. Proven mitigation strategies have been developed and documented. The primary areas of ES&H concern are listed below. A more detailed analysis for the Muon Beamline components is covered, along with the rest of the project, in the Mu2e Preliminary Hazard Analysis Document [15].

Radiation

The high intensity and high energy initial proton beam that hits the production target located in the PS bore is the primary source of radiation that will directly and indirectly (through secondary particles) irradiate the Muon Beamline components. Although the highest radiation dose will be accumulated in the PS side, all other Muon Beamline components will be exposed to a sufficiently high dose that proper radiation safety procedures will be required throughout the life of the project.

Pressure Safety

The Muon Beamline is essentially a large vacuum space formed by the bore of the solenoid system. Vacuum vessels pose a potential hazard to equipment and personnel from collapse, rupture or implosion. This danger is greatest near the thin windows that are required by the Mu2e experiment. Proper hazard and failure mode analysis will be performed to avoid the risk of generating vacuum failure.

Very heavy objects

Many of the Muon Beamline components (e.g., solenoid enclosures) are very heavy. There are significant mechanical hazards associated with the transport of heavy objects from one location to another. The Muon Beamline components will be moved by crane and by guide rails within the detector enclosure.

The potential consequences of mechanical hazards include serious injury or death to equipment operators and bystanders, damage to equipment, and interruption of the program. These hazards could be initiated by a dropped or shifted load, equipment failure, improper procedures or insufficient training/qualification of operators.

A hazard risk assessment will be conducted to evaluate the specific hazards to personnel for each of these activities and determine the means to mitigate the hazards. Any support structure that must carry over 10 tons will be reviewed for adherence to standard Fermilab engineering practices. Special lifting fixtures and transports will be designed for use with the solenoids. All lifting fixtures will be engineered, fabricated, and tested in accordance with ANSI/ASME Standard B30.20 (*Below-the-Hook Lifting Devices*). All applicable Fermilab design standards governing lifting devices will also be met. The maximum allowable lifting load will be legibly marked on each fixture. Sufficient space will be available inside the enclosures for personnel to remain clear of all lifting operations. Crane training, crane interlocks, inspections, and periodic maintenance will follow the procedures listed in the Fermilab ES&H Manual (FESHM). Personnel requiring authorization to use material handling devices must complete laboratory specified training and pass a qualification practical exam conducted by a skilled operator.

Electrical Hazards

High voltage and current are required to operate the Mu2e detectors. Since the Muon Beamline is responsible for providing the electrical feed-through ports, it is also exposed to electrical hazards. Electrical hazards include the potential for serious injury, death, and equipment damage. Electrical shock due to high voltage can be caused by exposed connectors, defective or substandard equipment, lack of adequate training, or improper procedures.

The electrical systems used to power the Mu2e solenoids and the hazards associated with them are similar to those in other experimental areas at Fermilab. Power distribution systems for the detectors will be designed in strict compliance with applicable codes. All systems will be grounded. Particular care will be provided for cable distribution to ensure code compliance with cable tray loading and content requirements. All electrical equipment, cables and cable trays will be protected against mechanical hazards according to established Fermilab ES&H procedures.

8.8 R&D Plan

WBS 5.2 Vacuum system

An R&D Test Vessel is proposed to test and verify all critical elements of the Muon Beamline Vacuum System. The general layout and components for the R&D Test Vessel are shown in Figure 8.42. The pumps, valves, and compressors shown are the actual ones specified for the experiment and will be used when Mu2e is assembled for production.

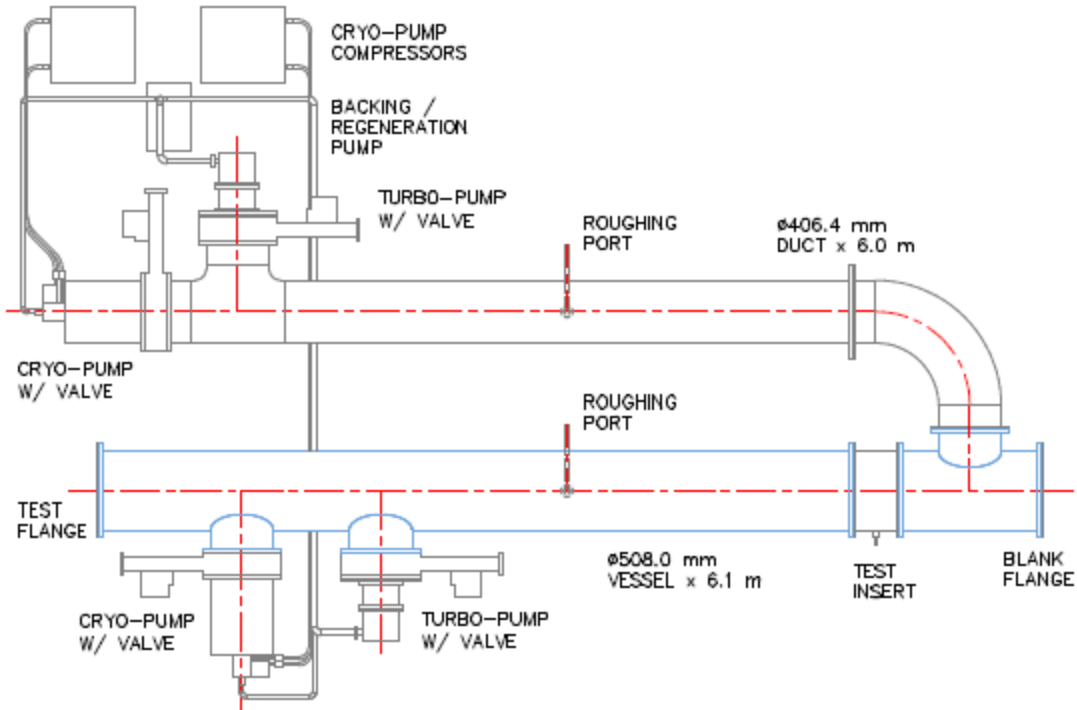


Figure 8.42. Configuration 1 of the Beamline Vacuum System R&D Test Vessel

The R&D Test Vessel is designed with flexibility to accomplish a large number of tests. The Configuration 1 apparatus shown can be used to verify the applicability and performance of the selected vacuum pumps. If the Vessel side pump valves are closed, the Duct side pumps will simulate and verify the conductance and pump-down performance of the PS + TSu vacuum system. In this configuration, the Test Insert is merely a through pipe, and the Test Flange is merely a blank flange.

If the Duct side pump valves are closed, the Vessel side pumps will simulate and verify the conductance and pump-down performance of the TSd + DS vacuum system. The Vessel can be loaded with a volume of outgassing material proportional to that found in the DS. In this configuration, the Test Flange is merely a blank flange and the Test Insert a through pipe, but a port on the Test Insert will allow the influx of a test gas. A proportional volume of tracker gas may be introduced to simulate straw leakage. Voltage breakdown measurements may be performed for the selected detector gases as a function of gas pressure by inserting a special High Voltage spark gap into the vacuum chamber. Air, water vapor, helium, or any combination of gases may be introduced to simulate any leakage or out-gassing effect.

The Configuration 2 apparatus, shown in Figure 8.43, can be used to verify the performance of the two most critical vacuum windows specified for Mu2e. In this configuration, the blank Test Flange is replaced by a 500 mm diameter Titanium

window assembly, and the through Test Insert is replaced by one with a Kapton antiproton window assembly and a series of bypass valves and piping installed. The Test Insert may be fitted with optical viewing ports to allow visual monitoring of the antiproton window.

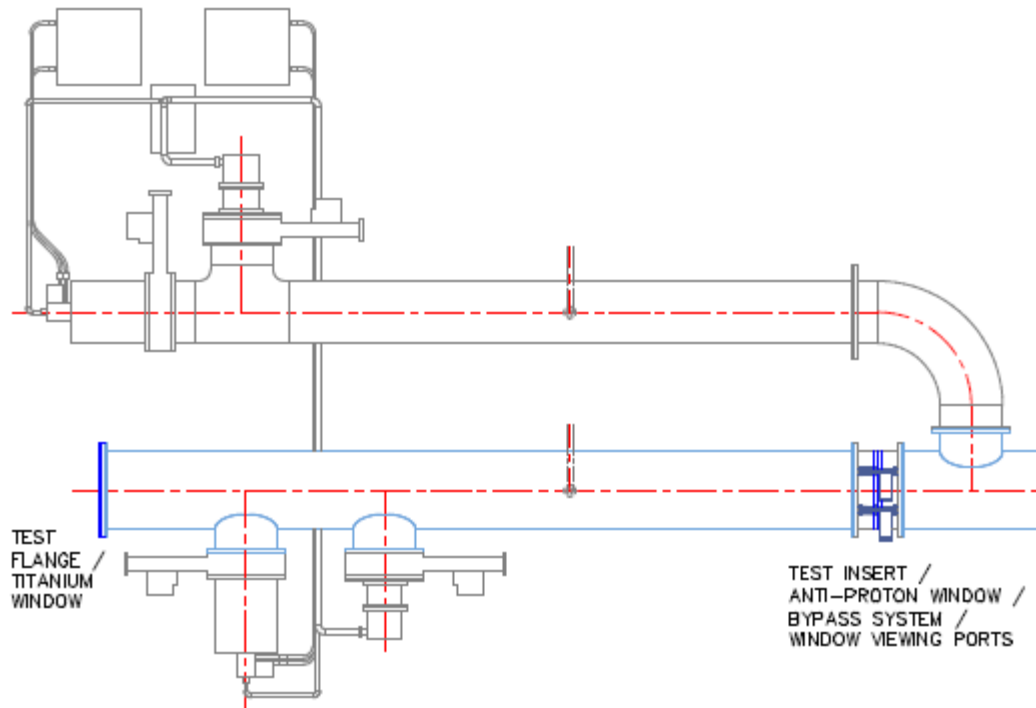


Figure 8.43. Configuration 2 of the Beamline Vacuum System R&D Test Vessel

In this configuration both the Duct side and Vessel side pump valves are open and all four pumps are in operation. One test will verify the performance of the bypass system and its associated control system in protecting the antiproton window from high differential pressures. The antiproton window may also be purposely subjected to high differential pressure to observe if failure occurs.

In this configuration, the largest PS Enclosure Titanium vacuum window can also be tested to ensure it survives the normal operating condition of 1 atm. differential pressure. Suitable ES&H restrictions will be maintained to ensure that no personnel are allowed near the Test Flange in case of Titanium window failure. In addition, a controlled failure of the Titanium window may be initiated to verify that the antiproton window survives the pressure wave produced in this kind of failure, and that the control system effectively shuts down the vacuum pumps. Mesh filters will be installed to protect the equipment from the potential of Titanium debris during a catastrophic window failure.

WBS 5.3 Collimators

Build and test a prototype drive mechanism for Col 3 to study the functionality of the collimator rotating mechanism, particularly the operational behavior of the electric motor under cryostat vacuum conditions.

Development of the antiproton stopping window design including:

- Window material selection and design.
- Window mounting and sealing design.
- Operational and failure pressure tests.

This work will be coordinated with the Vacuum System R&D efforts under WBS 5.2.

WBS 5.4 Muon Beamline Shielding

External Shielding Design:

- Study of the external shielding materials and alternate designs.
- Prototype development for an easily assembled and movable shielding system.

WBS 5.5 Stopping Target and WBS 5.6 Proton Absorber

Build prototype stopping target and proton absorber with their support structures. Verify that positioning and alignment tolerances can be met.

WBS 5.7 Stopping Target Monitor

The stopped muon rate in Mu2e is obtained by monitoring the rate of muonic xray production in the stopping target. At the same time, a major source of background comes from the muon capture process, where protons, neutrons and gamma rays are emitted in quantity. To verify the feasibility of this concept of monitoring the muon cascade and the rate of secondary production in the capture process, we need to perform a series of tests using a low energy muon beam. To verify the monitoring process, we propose to utilize the same Germanium detector (part of STM) as is planned to be used in the Mu2e experiment. The fluxes of secondary protons and neutrons will be monitored with silicon detectors and neutron detectors, respectively, while high energy photons will be monitored with a sodium iodide detector. It will be difficult to find a large solenoid system to use for the tests so the tests very likely will not be performed under the influence of the magnetic field. We might also be limited in our ability to obtain the right bunch structure for the muon beam. Nevertheless the results we obtain will be essential to properly predict how the ST and the STM will work under the Mu2e experimental conditions. An additional simulation effort – to

predict STM behavior under Mu2e experiment conditions based on the obtained test data – will be also included in this plan.

Two distinct periods of tests are envisioned:

1. Tests at TRIUMF
2. Tests at PSI

Tests at TRIUMF

Osaka University plans to obtain beam time at TRIUMF and we will join them to perform the following tests:

- Measuring the muon beam flux
- Measuring the X-ray spectra from different target material
- Measuring high energy photon spectra

Tests at PSI

The PSI (Paul Scherrer Institut, Villigen Switzerland) test can be divided into three phases:

- Test Preparation
- Data taking at PSI
- Offline Data Analysis

Test Preparation

In this phase we will procure the ST and STM detector including the readout system that allows us to collect and record the data. We also need to work out the interface issues with PSI to make sure that the proper infrastructure is present for our equipment.

Data Taking at PSI

In this phase we will travel to PSI and perform the following measurements:

- Measure muon flux via muonic X-rays and beam counters
- Measure proton flux
- Measure neutron flux
- Measure gamma flux and delayed gamma flux
- Measure high energy (above 100 MeV) photon flux.
- Repeat for stopped pions.

To perform these measurements we need to spend 3 weeks at the PSI facility.

Offline Data Analysis Effort

Most of the effort will be done back at the home institutions where the infrastructure is well established so we don't expect any additional M&S expenses.

The offline analysis will include:

- Processing the raw data
- Extracting capture signal rates and background rates
- Estimating capture rates at Mu2e experimental setup

WBS 5.8 Muon Beam Stop

- Simulations will be completed to determine the type and level of doping of HDPE parts.
- Simulations will be completed to determine the level of magnetic permeability that can be accepted from the stainless support ring. If slightly higher levels of permeability can be accepted, 304 rather than 316 stainless can be used, decreasing cost.
- Sample HDPE parts will be fabricated to ensure tolerances can be held.
- A larger ring (short mockup of the stainless ring) will be built and assembled with the HDPE rings to understand fit and shimming of HDPE parts within the stainless ring.
- Calculations will be completed to ensure the beam stop will not deflect excessively under its own weight and that the support structure for the beam stop is structurally adequate.

WBS 5.9 Neutron Absorbers

- The current design utilizes concrete blocks with reinforcement bars of magnetic steel. Studies will determine whether the location of the magnetic bars will be acceptable with regard the DS field quality and/or will have structural issues due to eddy currents. If field quality is an issue, stainless steel bars are available, at a higher cost.

WBS 5.10 Detector Support and Installation System

- Structural calculations of the entire system, internal and external, will be completed and documented to ensure the structural adequacy of the system.
- Simulations will be completed to determine the level of magnetic permeability that can be accepted from the rail system components. If slightly higher levels of permeability can be accepted, some alternate materials may be used, decreasing costs.

- Analysis will be done to ensure that temperature variations within the DS bore do not cause binding or other problems associated with the rail system, to a degree that causes the alignment specifications to be violated.
- Critical support elements will be purchased and tested to prove the concept of both the internal and external rail system. These will include a section of the rail system at least 3 meters long, made out of standard magnetic material, as well as at least 4 bearing blocks. The “mockup” rails can be re-used as the external system for the actual installation, recouping the money spent for these parts.
- This system will be set up at a location in the Industrial Area at Fermilab, and mockups of critical components will be placed on them with their support structures, aligned, and realigned, using the proposed alignment system, to test wherever possible through “dry run”, the entire assembly procedure, and to verify that the specified tolerances on placement can be achieved.
- Two small sections of rail will be fabricated, attached and tested to ensure that this connection can be made adequately.
- In the actual DS bore, the rail system will be supported by a set of stainless steel supports to be welded to the inner wall of the DS cryostat. As part of the R&D plan, a section of stainless steel, the same thickness as the DS inner wall, will be welded to a mockup of the supports by the same process proposed for the actual supports. Measurements of distortion and magnetic permeability will be taken before and after welding to ensure that the welding process does not cause a violation of the DS specifications.

8.9 References

- [1] J. Brandt B. Norris and J. Popp, “Requirements and Specifications Document, WBS 5.2, Beamline Vacuum System,” Mu2e-doc-1481.
- [2] N. Andreev, “Requirements and Specifications Document, WBS 5.3, Collimators,” Mu2e-doc-1044.
- [3] N. Andreev et al., “Requirements and Specifications Document, WBS 5.4, Beamline Shielding,” Mu2e-doc-1436.
- [4] T. Ito, “Requirements and Specifications Document, WBS 5.5, Stopping Target,” Mu2e-doc-1437.
- [5] T. Ito, “Requirements and Specifications Document, WBS 5.6, Stopping Target Monitor,” Mu2e-doc-1438.
- [6] T. Ito, “Requirements and Specifications Document, WBS 5.7, Proton Absorber,” Mu2e-doc-1439.
- [7] R. Bossert, “Requirements and Specifications Document, WBS 5.8, Muon Beam Stop,” Mu2e-doc-1351.

- [8] R. Bossert, "Requirements and Specifications Document, WBS 5.9, Neutron Absorber," Mu2e-doc-1371.
- [9] R. Bossert, "Requirements and Specifications Document, WBS 5.10, Detector Support and Installation System," Mu2e-doc-1383.
- [10] S. Feher, "Requirements and Specifications Document, WBS 5.11, System Integration, Tests and Analysis," Mu2e-doc-1168.
- [11] M. Dinno, "Risk Registry," Mu2e-doc-1463.
- [12] S. Feher, "Quality Assurance Plan for the Muon Beamline sub-project of the Mu2e Experiment," Mu2e-doc-1471.
- [13] D. Hedin, "Muon Beam Stop Update", presented at Mu2e collaboration meeting, Jan 28, 2012, Mu2e-docdb-2003.
- [14] J. Popp and M. McKeown, "Vacuum Studies II", Mu2e-doc-1267.
- [15] R. Ray, "Preliminary Hazard Analysis Document," Mu2e-doc-675.